

# Evaluation and projections of extreme precipitation using a spatial extremes framework

Lichao Yang<sup>1</sup>  | Christian L. E. Franzke<sup>2,3</sup>  | Wansuo Duan<sup>1,4</sup> 

<sup>1</sup>State Key Laboratory of Numerical Modeling for Atmospheric Sciences and Geophysical Fluid Dynamics, Institute of Atmospheric Physics, Chinese Academy of Sciences, Beijing, China

<sup>2</sup>Center for Climate Physics, Institute for Basic Science, Busan, South Korea

<sup>3</sup>Pusan National University, Busan, South Korea

<sup>4</sup>University of Chinese Academy of Sciences, Beijing, China

## Correspondence

Christian L. E. Franzke, Pusan National University, Busan, South Korea.  
 Email: [christian.franzke@pusan.ac.kr](mailto:christian.franzke@pusan.ac.kr)

## Funding information

Institute for Basic Research, Grant/Award Number: IBS-R028-D1; National Nature Scientific Foundation of China, Grant/Award Number: 42105061; National Research Fund of Korea, Grant/Award Number: NRF-2022M3K3A1097082

## Abstract

Extreme precipitation events are a major natural hazard and cause significant socio-economic damages. Precipitation events are spatially extended and, thus, can cause large water accumulations, which can lead to flooding events. In order to help design flood protection infrastructure, a detailed investigation of the temporal and spatial dependencies of extreme precipitation is essential. Here, we use a statistical spatial extremes framework to systematically study the historical and projected spatial-temporal characteristics of extreme precipitation in Germany. For this purpose, we use data from 10 high-resolution global climate model-regional climate model (GCM-RCM) combinations from the EURO-CORDEX initiative and derive a statistical spatial extremes precipitation model. Our results show that there are large spreads in reproducing the temporal-spatial characters of extreme precipitation. Few climate simulations can well present the temporal clustering of observed extreme precipitation in both summer and winter. In reproducing the spatial dependencies of the observations, most GCM-RCM combinations behave well in summer, while in winter most RCMs produce too many spatially localized extreme precipitation events. The derived statistical model, which accounts for both the spatial and temporal variability, performs well in representing the spatial dependency and intensity characteristics in summer. Furthermore, global warming will have a significant impact on the temporal and spatial dependencies of extreme precipitation in Germany. There will be more temporal-dependent and homogeneous extreme precipitation in summer; and more temporal-independent and localized extreme precipitation in winter. The intensity quantified by the 25-year return level of the 10 GCM-RCM combinations is increasing; with relative changes ranging from 5.33% to 53.24% in summer and from -15.38% to 32.33% in winter under RCP8.5. A future projection by

This is an open access article under the terms of the [Creative Commons Attribution-NonCommercial License](#), which permits use, distribution and reproduction in any medium, provided the original work is properly cited and is not used for commercial purposes.

© 2023 The Authors. *International Journal of Climatology* published by John Wiley & Sons Ltd on behalf of Royal Meteorological Society.

our statistical spatial extremes model using projected temperature from GCM-RCM combinations as a covariate shows that the 25-year return level will increase by 3.02% under RCP2.6 and 4.16% under RCP8.5 in winter.

#### KEY WORDS

extreme precipitation, max-stable model, model evaluation, spatial extremes

## 1 | INTRODUCTION

Extreme precipitation events are of great concern due to their direct impact on humans, infrastructure and ecosystems (Franzke, 2017, 2021; Franzke & Torelló i Sentelles, 2020; Hallegatte et al., 2013; Masson-Delmotte et al., 2021; Merz et al., 2010). How the characteristics of extreme precipitation changes with global warming is of significant social concern, with rainfall-driven floods being one of the most costly natural hazards worldwide. Although numerous studies have shown the intensification of heavy precipitation events with climate change, there is a wide variety of intensification changes in different regions (Donat et al., 2016; O'Gorman & Schneider, 2009; Zeder & Fischer, 2020). A detailed description of extremal statistics of precipitation in specific regions will be more helpful for local governments to support city planning policies and design flood protection infrastructure.

Global climate models (GCMs) have been used as an efficient way for studying the historical and projected future changes in climate extremes. However, extreme precipitation simulated by GCMs is often not adequately reproduced because of their coarse grid resolution and their subsequent need of parameterizations, which lead to the misrepresentation of physical processes, (van der Wiel et al., 2016; Wang et al., 2014). High-resolution regional climate models (RCMs), which possess higher resolution and resolve better physical and dynamical processes, have shown an improved capability in reproducing extreme precipitation, especially over Europe (Ehmele et al., 2020; Sunyer et al., 2016). Recently, the EURO-CORDEX historical and future projection simulations have been provided as part of the European Copernicus Climate Change Service (C3S), resulting in 0.11°-resolution climate simulations (Jacob et al., 2020). This offers the possibility of more reliable projected climate simulations.

Besides dynamical climate models, statistical models are also an efficient way to study extreme precipitation. Without involving the complexity of physical processes, statistical models aim to generate surrogate time series, resembling the observed statistical and spatial characteristics of extreme precipitation. Many statistical processes are available to model extreme precipitation, such as the fractional Poisson process, copula-based processes and

the max-stable process (Hannachi, 2014; Kim & Onof, 2020; Paschalis et al., 2013; Yang, Franzke, & Fu, 2020; Yang, Franzke, & Fu, Z., 2020). It has been shown that statistical models are competitive in modeling extreme precipitation (Yang, Franzke, & Fu, 2020). Moreover, by adding a time-dependent covariate in the statistical model, these models might also be able to generate projected extreme precipitation, which has the potential to serve as a complementary approach for climate impact studies.

Dynamical and statistical models are both useful tools to study the characteristics of extreme precipitation. In order to get reliable projections of extreme precipitation, evaluation of how well the models simulate historical extreme precipitation is necessary. In many previous studies, climate extreme indices (Expert Team on Climate Change Detection and Indices, ETCCDI), suggested by Zhang et al. (2011), including the percentile-based intensities and durations of an event, are computed to characterize extreme precipitation (Alexander & Arblaster, 2017; Dosio & Fischer, 2018).

However, in order to get a detailed description of the extreme precipitation characteristics in a region, it is not sufficient to only summarize extremes in terms of magnitudes and durations. For example, extreme precipitation events can occur in close succession; potentially delivering large precipitation accumulations. Moreover, a large spatial extent of extreme precipitation events can be hazardous, as it can trigger a larger surface runoff response, which increases the risk of flooding and landslides (Barton et al., 2016; Martius et al., 2013). Although previous studies have analysed the statistical properties and dynamical contributions of temporal clusters of historical extreme precipitation events, namely the extreme precipitation in the mid-western region of North America (Villarini et al., 2011) and southern Switzerland (Barton et al., 2016), it has not been studied widely how well climate models reproduce the temporal clustering of extreme precipitation and how it changes with global warming.

Furthermore, since extreme precipitation events do not occur at a single point, there would be a clear spatial dependence of extreme intensities at short or medium distances. A stronger spatial dependence means there is a higher probability that the extremes at two close points occur

simultaneously. While a weaker spatial dependence indicates that the extremes are more localized. Studying the historical and projected spatial dependence of extreme precipitation is crucial for risk estimation and hydrological management over a certain region. So far, the spatial dependence has not been widely investigated and no study has investigated projected future trends of the spatial dependence of extreme precipitation as far as we are aware of.

In this study, we selected Germany, which has the second-largest population in Europe and regularly experiences flooding events, as our research region. It has a typical mid-latitude moderate climate, characterized by a western flow with abundant precipitation associated with frontal systems in winter and more convective precipitation in summer (Warrach-Sagi et al., 2013). We will investigate the temporal and spatial dependence of extreme precipitation and its projected future changes in the summer (JJA—June, July and August) and winter (DJF—December, January and February) seasons using 10 high-resolution GCM-RCM combinations and one statistical model over Germany. We will address the following research questions:

1. How well do dynamical and statistical climate models reproduce the temporal and spatial dependencies of daily extreme precipitation?
2. How will the temporal and spatial dependencies of extreme precipitation change under different future climate scenarios?

The use of these statistical extreme value methods provides us with new insights into the quality and accuracy of RCM outputs, and also helps us to study projected future climate change. The remainder of this paper is structured as follows. In Section 2, we describe the 1 km resolution observational dataset (HYRAS) and the 10 GCM-RCM combination simulations with a resolution of 0.11°. The Max-stable statistical model is described in Section 3, where we also introduce the statistical methods to quantify the temporal and spatial dependence of extremes. In Section 4, we evaluate the historical daily extreme precipitation of GCM-RCM combinations and the statistical model with the observations. In Section 5, we assess the future projections of extreme precipitation. Conclusions and discussions are given in Section 6.

## 2 | DATA

### 2.1 | The HYRAS gridded precipitation data set

The HYRAS gridded daily precipitation data set is provided by the Deutscher Wetterdienst (DWD) Climate

Data Center, covering Germany with a resolution of 1 km during the period of 1931 through 2021 and has been widely used in climate and hydrological studies ([https://opendata.dwd.de/climate\\_environment/CDC/grids\\_germany/daily/hyras\\_de/precipitation/](https://opendata.dwd.de/climate_environment/CDC/grids_germany/daily/hyras_de/precipitation/), Rauthe et al. (2013)). More than 5000 rainfall gauges are used for the HYRAS dataset, with the REGNIE interpolation method, in which a multiple linear regression is applied to create background fields of precipitation. The high-resolution dataset can provide more details of extreme precipitation variability (Hu & Franzke, 2020). Here, we study the observations during the time period 1961–2005.

### 2.2 | The RCM data sets

We use daily precipitation sums from a series of GCM-RCM combinations with a resolution of 0.11°, collected by the European Coordinated Regional Climate Downscaling Experiment program (EURO-CORDEX) (<https://esgf-data.dkrz.de/search/cordex-dkrz/>). To keep the consistence of the studying period with the observations period, we selected the period between 1961 and 2005 as the historical condition. To keep the same data length with the historical condition, for the future scenarios, we select two Representative Concentration Pathway (RCP 2.6 and 8.5) scenarios during the years of 2056–2100 (Gu et al., 2020; van Vuuren et al., 2011). According to the selection criteria, there are 10 GCM-RCM combinations available in the public archive. The list of GCMs, RCMs and modelling institutions are given in Table 1. To reduce the bias induced by the interpolating method (Zou et al., 2021), we choose the closest grid point of the observational data set to compare with the model simulations followed by Diaconescu et al. (2018) and Pendergrass and Knutti (2018).

## 3 | METHODS

### 3.1 | Generation of a spatial statistical model: The max-stable model

Multi-variate extreme-value distributions of a spatial model can be represented as a max-stable process (de Haan, 1984; de Haan & Pereira, 2006). The max-stable distribution is described as follows (Ribatet, 2017): Let  $X_1, X_2, \dots$  be a sequence of independent copies of a random variable vector  $X$ . If there exist normalizing sequences  $\{c_n > 0 : n \geq 1\}$  and  $\{d_n : n \geq 1\}$  such that

**TABLE 1** Summary of the global climate model-regional climate model (GCM-RCM) combinations used in the study.

GCM	RCM	Model name	Modelling institution
MPI-M-MPI-ESM-LR	REMO2009	MPIESM-REMO2009	MPI-CSC, Max-Planck Institute, Germany
MPI-M-MPI-ESM-LR	RACMO22E	MPIESM-RACMO22E	MPI-CSC, Max-Planck Institute, Germany
MPI-M-MPI-ESM-LR	RCA4	MPIESM-RCA4	MPI-CSC, Max-Planck Institute, Germany
NCC-NorESM1-M	REMO2015	NorESM-REMO2015	GERICS, Climate Service Center Germany
NCC-NorESM1-M	RACMO22E	NorESM-RACMO22E	KNMI, Royal Netherlands Meteorological Institute, Ministry of Infrastructure and the Environment, Netherlands
NCC-NorESM1-M	RCA4	NorESM-RCA4	SMHI, Swedish Meteorological and Hydrological Institute, Sweden
MOHC-HadGEM2-ES	HadRCM3-GA7-05	HadGEM2-HadREM3	MOHC, Met Office Hadley Centre, United Kingdom
MOHC-HadGEM2-ES	RCA4	HadGEM2-RCA4	SMHI, Swedish Meteorological and Hydrological Institute, Sweden
IPSL-IPSL-CM5A-MR	REMO2015	CM5A-REMO2015	GERICS, Climate Service Centre Germany, Germany
CNRM-CERFACS-CNRM-CM5	ALARO-0	CNRM-ALARO-0	RMIB-UGent, Royal Meteorological Institute of Belgium and Ghent University, Belgium

$$\frac{\max_{i=1,\dots,n} X_i - d_n}{c_n} \rightarrow Z, n \rightarrow \infty \quad (1)$$

in distribution, then provided it is non-degenerate, the random variable vector  $Z$  has a max-stable process. For multiple locations, the marginal distribution of the variable  $Z$  are generalized extreme value (GEV) distributed with different location, scale and shape parameters. Different from the spatial GEV models, the max-stable model permits spatial dependence. Recently, pairwise likelihood fitting methods have been developed, paving the way into the generation of max-stable models (Ribatet, 2017; Westra & Sisson, 2011). Based on the spectral representation of the max-stable process, there are three steps for modelling the spatial extremes using a max-stable model (Ribatet, 2009):

### 1. Modelling the spatial dependence

We transform each annual maximum precipitation series  $Y$  into unit-Frechet margin series  $Z$  (GEV [1,1,1]) by Equation (2):

$$Z = \left[ 1 + \xi \frac{Y - \mu}{\sigma} \right]^{\frac{1}{\xi}}, \quad (2)$$

where  $\mu$ ,  $\sigma$  and  $\xi$  are the location, scale and shape parameters. Then the  $Z$  series over the region are fitted by a two-dimensional spatial statistical model by using the

**TABLE 2** Specific expressions of the spatial dependence models.

Model	Expression
Schlather	$\{Y_i(x) : x \in \chi\} = \sqrt{2\pi} \max\{0, \epsilon(x)\} : x \in \chi$
Extremal- $t$	$\{Y_i(x) : x \in \chi\} = \{c_\nu \max\{0, \epsilon(x)\}^\nu : x \in \chi\}, c_\nu = \sqrt{\pi} 2^{-\frac{\nu-2}{2}} \Gamma(\frac{\nu+1}{2})$
Brown-Resnick	$\{Y_i(x) : x \in \chi\} = \{\exp\{\epsilon(x) - \gamma(x)\}, x \in \chi\}, \gamma(x) = (x/\lambda)^\alpha$
Smith	$\{Y_i(x) : x \in \chi\} = \{\exp\{\epsilon(x) - \gamma(x)\}, x \in \chi\}, \gamma(x) = (x/\lambda)^2$

pairwise likelihood method (Ribatet, 2009). Here, we test the Smith model, the Schlather model, the extremal- $t$  model and the Brown–Resnick model to see which model fits the data best. Different models will give different spatial structures. The specific expression for each model is displayed in Table 2. The fitting procedure is explained in detail by Ribatet (2017). To select the best model for representing the spatial structure of extreme precipitation, we calculate the Takeuchi Information Criterion (TIC) value of each model, which is suitable for the model under misspecification (Ribatet, 2009; Varin & Vidoni, 2005). The model with the minimum TIC can be considered as the best model to reproduce the spatial dependence structure of the series  $Z$  over the region.

### 2. Modelling the Marginal Distribution

The marginal distribution of each  $Y$  is modelled by a spatial GEV distribution. Specifically, in each grid  $(x)$ ,

we fitted the series  $Y(x)$  with the GEV distribution where  $\mu(x), \sigma(x), \xi(x)$  are the location, scale and shape parameters, respectively. These parameters are modelled dependent on the longitude ( $lon(x)$ ), latitude ( $lat(x)$ ) of each grid and the seasonal mean temperature of Germany ( $T$ ) (Equation (3)). The maximum-likelihood method is used for estimating the parameters and the best model is chosen by the minimum TIC value as well.

$$\begin{aligned}\mu(x, T) &= \beta_0^0 + \beta_1^0 lon(x) + \beta_2^0 lat(x) + \beta_3^0 T \\ \sigma(x, T) &= \beta_0^1 + \beta_1^1 lon(x) + \beta_2^1 lat(x) + \beta_3^1 T \\ \xi(x, T) &= \beta_0^2 + \beta_1^2 lon(x) + \beta_2^2 lat(x) + \beta_3^2 T\end{aligned}\quad (3)$$

### 3. Joint Modelling

After we determined the best models for both spatial dependence ( $Z'$ ) and marginal distribution (GEV ( $\mu', \sigma', \xi'$ )), we combine the two models by the inverse function of Equation (2). Then, we are able to generate the statistical extreme precipitation model ( $Y'$ , Equation (4)) which preserves the same spatial dependence and the marginal distributions over Germany.

$$Y'(x) = \frac{\sigma'(x)(Z'(x)^{\xi'(x)} - 1)}{\xi'(x)} + \mu'(x) \quad (4)$$

### 3.2 | The spatial dependence coefficient

To quantify the spatial dependence between two grid points, a common method is the (semi) variogram in geostatistics. However, when working with extreme values, the variogram is not a useful tool since the variogram of simple max-stable processes may not exist. As a substitute to the (semi) variogram, here we use the extremal coefficient ( $\theta$ ) based on the  $F$ -madogram, proposed by Cooley et al. (2006). It can better reflect the spatial dependence between extremes and has been used as an effective tool to quantify the spatial dependence (Hu & Franzke, 2020; Yang, Franzke, & Fu, 2020). The extremal coefficient is defined by,

$$\hat{\theta}(x_1 - x_2) = \frac{1 + 2\nu_F(x_1 - x_2)}{1 - 2\nu_F(x_1 - x_2)}. \quad (5)$$

where

$$\nu_F(x_1 - x_2) = \frac{1}{2n} \sum_{i=1}^n \left| \left( F(z_i(x_1)) - F(z_i(x_2)) \right) \right|, \quad (6)$$

$$F(z) = \exp(-1/z). \quad (7)$$

$Z(x)$  is a stationary max-stable random field with unit Frechet margins.  $z_i(x_1)$  and  $z_i(x_2)$  are the  $i$ -th observations of  $Z(x)$  at locations  $x_1, x_2$  and  $n$  is the total number of observations. The extremal index lies between 1 and 2.  $\hat{\theta}=1$  denotes the observations at two grid points that are totally spatially dependent and  $\hat{\theta}=2$  means the two observations are spatially independent.

### 3.3 | The temporal extremal index

The extremal index is a useful indicator of how much temporal serial clustering of exceedances of a threshold occurs in the limit of the distribution. Various estimators have been applied for the extremal index (Ferreira, 2018; Kopp et al., 2021; Moloney et al., 2019). Here, we adopt the ‘runs’ method, one of the simplest but widely used ways of estimating the extremal index, proposed by Coles (2001). In the precipitation time series, we define the 90th percentile as the threshold and count the number of extremes exceeding the threshold ( $n_u$ ). The successive extremes should be defined as a cluster. Pragmatically, the extremes might be interrupted by a short pulse (Bernardara et al., 2007). So in the runs method the cluster is taken as terminated when the series stayed below the threshold for at least  $r_c$  steps. In this study, we define the  $r_c$  as three steps and count the number of clusters ( $n_c$ ). The extremal Index is computed by dividing the number of clusters  $n_c$ , by the number of exceedances  $n_u$

$$\hat{\kappa} = \frac{n_c}{n_u} \quad (8)$$

The  $\hat{\kappa}$  has a value range from 0 to 1.  $\hat{\kappa}=1$  means the extremes are independent, which means all clusters are composed solely of a single extreme.  $\hat{\kappa}<1$  indicates that the extremes appear in clusters and there is temporal dependency between the extremes. The smaller  $\hat{\kappa}$  means there are more clustered extremes.

### 3.4 | Return levels of the extremes

In hydrological studies, return levels and periods are widely used to describe and quantify risks of extremes.

Following Laflamme et al. (2016), here we use the 25-year return level as an indicator to evaluate the extreme magnitudes simulated by the GCM-RCM combinations and the statistical model. For each dataset, seasonal maxima at each grid are first fitted to the GEV distribution by the maximum likelihood method. The 96th quantile value of the fitted GEV distribution is defined as the 25-year return level of each grid.

The performance of each simulation in reproducing the extreme precipitation character over the study region is evaluated using the root-mean-squared-error (RMSE). Taking the 25-year return level as an example, the RMSE defined as

$$\text{RMSE} = \left[ \frac{1}{K} \sum_{n=1}^K (e_{m,n} - e_{o,n})^2 \right]^{1/2} \quad (9)$$

where,  $e_{m,n}$  and  $e_{o,n}$  represent the 25-year return levels at grid point  $n$  in the model and the closest corresponding observation grid point  $o$ , respectively.  $K$  is the total number of grid points over Germany. The evaluations on the spatial dependence (using extremal coefficient introduced in Section 3.2) and temporal cluster (using extremal index introduced in Section 3.3) are quantified in similar ways by RMSEs. Besides the RMSE, the spatial correlation is also applied in the evaluation.

## 4 | OBSERVED RESULTS AND MODEL EVALUATION

In this section, we evaluate the historical temporal and spatial dependencies, return levels of extreme precipitation generated by GCM-RCM combinations and the max-stable model.

### 4.1 | Temporal dependence of extreme precipitation

Figure 1 shows the temporal extremal index of HYRAS and of all GCM-RCM combinations, as well as the multi-model mean in summer and winter. The observed extremes tend to appear more independently in summer ( $\bar{\kappa}=0.87$ ), while they tend to occur more clustered in winter ( $\bar{\kappa}=0.63$ ). This is a result of different types of precipitation. In summer, most of the extreme precipitation is caused by convective systems, which usually tend to occur independently from each other. While in winter, extreme precipitation is mostly induced by the large-scale circulation and often lasts for several days.

In summer, the clustered extreme precipitation events tend to occur in the northern and central part of Germany. There is a considerable spread in this statistic across different climate model simulations, as most models show an underestimation of serial clustering compared with the observations, especially the models driven by MPIESM and NorESM1 (see Figure 1). While for the RCMs driven by HadGEM2, there is an obvious overestimation of the clustering in the western and southern part of Germany. The RCMs driven by CM5A behave relatively well in reproducing the serial clusters, with the spatial correlation of 0.21 and 0.24 in the CM5A-REMO2015 and CM5A-ALARO-0 simulations, respectively. The CM5A-ALARO-0 simulation also present the lowest RMSE among the 10 GCM-RCM combinations (see Table 3). Both the GCM and RCM influence the temporal cluster of extremes in the simulations. The selection of the GCM tend to impact the sign of the differences between the simulations and observations (see Figure 1). For example, the RCMs driven by MPIESM show an overall overestimation of the extremal index and the RCMs driven by HadGEM2 tend to present an underestimation of the index. The MPIESM-RCA4 and HadGEM2-RCA4 simulations, which are sharing the same RCM but are driven by different GCMs, show opposite differences in the extremal indices. The selection of the RCM tend to impact the details of the geographical distribution of the extremal index, since there are large differences of spatial correlations in the simulations that have the same GCMs but different RCMs (see Table 3). So both the GCMs and RCMs have significant impacts on simulating the temporal cluster of extreme precipitation in summer. The multi-model mean could largely capture the features seen in southern Germany, but underestimates the extremal index in the northwest.

In winter, the observed clustered extreme precipitation events tend to occur in western Germany. Each climate model simulation shows a large deviation from the observed extreme clustering. Most climate model simulations present higher temporal extremal indices across Germany, which means the extreme precipitation simulated by GCM-RCM combinations tend to occur more independently than observations. In particular, for the CM5A-REMO2015 simulation, there is an underestimation of serial clustering across the whole of Germany. The HadGEM2-HadREM3 and CM5A-ALARO-0 are the two simulations that perform the best in characterizing the observed temporal cluster behaviour, with spatial correlations of 0.41 and 0.33. Though the HadGEM2-HadREM3 shows higher spatial correlations, it underestimates the clustering characteristics in western Germany, so that the RMSE is larger than the CM5A-ALARO-0 simulation (see

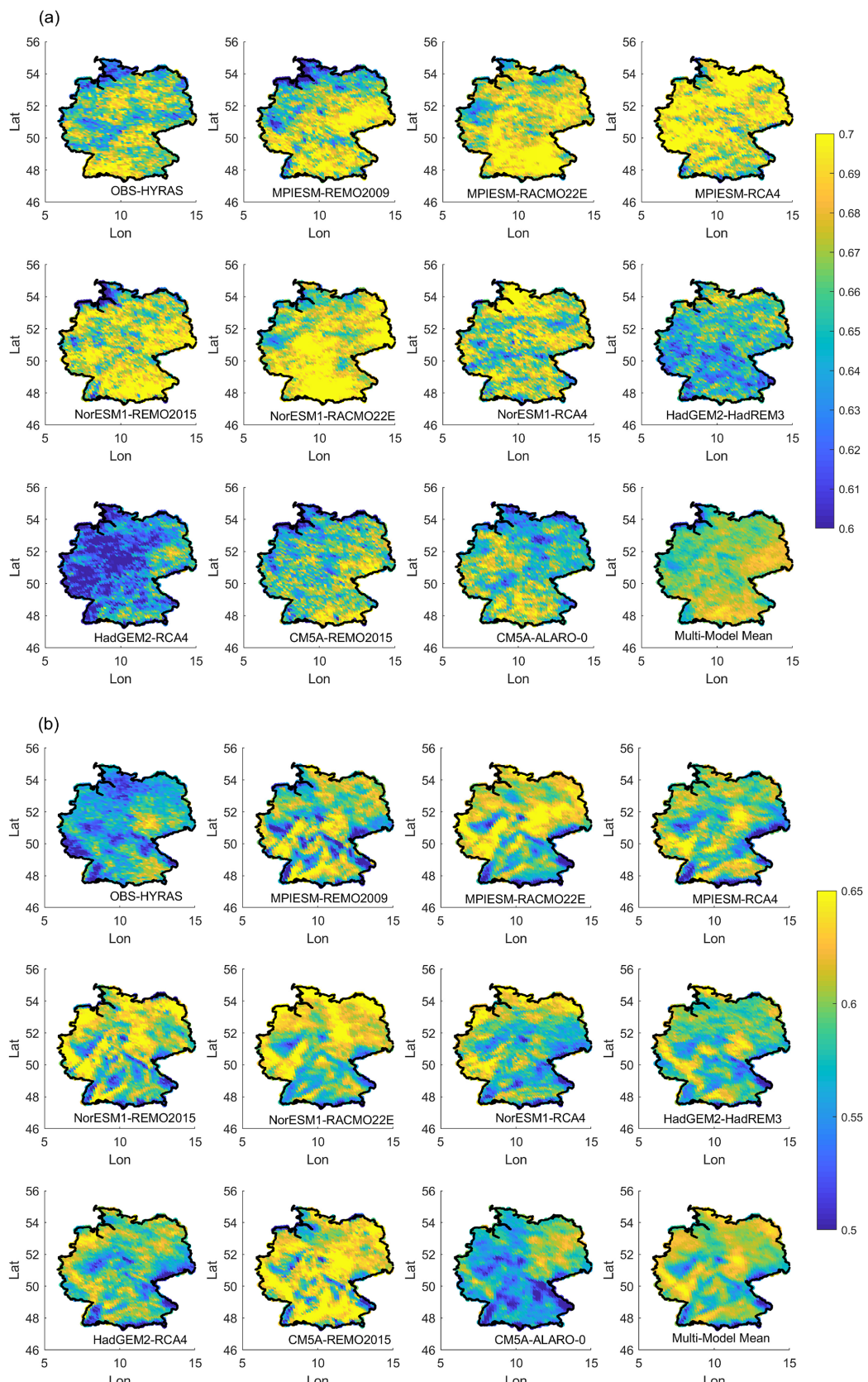


**FIGURE 1** Geographical distributions of the extremal indexes of observations and climate model simulations in (a) summer and (b) winter. [Colour figure can be viewed at [wileyonlinelibrary.com](http://wileyonlinelibrary.com)]

TABLE 3 Spatial Correlations of the temporal extremal index between climate model and observation.

Season	R1	R2	R3	R4	R5	R6	R7	R8	R9	R10
Summer	<b>0.23</b> (0.035)	0.18 (0.034)	-0.07 (0.042)	0.22 (0.037)	0.20 (0.037)	-0.09 (0.036)	-0.04 (0.036)	0.11 (0.053)	0.21 (0.039)	<b>0.24</b> (0.029)
Winter	-0.02 (0.060)	0.18 (0.061)	0.23 (0.051)	-0.05 (0.067)	0.13 (0.064)	-0.04 (0.055)	<b>0.41</b> (0.042)	0.24 (0.046)	0.24 (0.070)	<b>0.33</b> (0.038)

Note: The root-mean-squared-error (RMSE) of each climate model is shown in brackets. The best two models are marked in bold. R1:MPIESM-REMO2009, R2: MPIESM-RACMO22E, R3:MPIESM-RCA4, R4:NorESM1-REMO2015, R5:NorESM1-RACMO22E, R6:NorESM1-RCA4, R7:HadGEM2-HadREM3, R8: HadGEM2-RCA4, R9:CM5A-REMO2015, R10:CM5A-ALARO-0.

Table 3). The GCMs and RCMs both influence the temporal cluster of extreme precipitation in winter. In particular, the CM5A-REMO2015 and CM5A-ALARO-0 simulations, which have the same GCM but different RCMs, show totally different extremal indices (see Figure 1). Though the MPIESM-RCA4, NorESM-RCA4 and HadGEM2-RCA4 have the same RCM, their spatial correlations with the observations are 0.23, -0.04 and 0.24, respectively (see Table 3). Different from the results in summer, the multi-model mean cannot reproduce the spatial characteristics of the extreme clustering well in winter. It shows more independent extremes, especially in the western part. Previous studies have shown that the temporal clustering characteristics of extreme precipitation is associated with large-scale climate modes, such as the Arctic Oscillation (AO) and the North Atlantic Oscillation (NAO) (Yang & Villarini, 2019). An improvement of simulating the large-scale climate modes in climate models may help improve the capabilities in simulating the temporal clusters of extreme precipitation. Nevertheless, how to improve the capabilities of climate model simulations on temporal cluster of extreme precipitation still needs further studies.

## 4.2 | Spatial dependence of extreme precipitation

To show the spatial dependence over the whole region, we compute the distribution of the extremal coefficients over all pairs of grid points. Figure 2 compares the distribution of the mean and the uncertainty of the extremal coefficients as a function of pairwise distances in observations and GCM-RCM combinations in summer and winter. As expected, as the distance between two grid points increases, the spatial dependence becomes weaker. Compared with the observed extremes in summer, the  $\theta$  values in winter decrease, which means the spatial dependence of extremes in winter is stronger. This may be related to the different types of extreme precipitation events in different seasons. In summer most of the

extreme precipitation events are caused by localized convective systems, while in winter extreme events are more likely caused by large-scale systems, so that the extreme magnitudes are more spatially dependent. It is consistent with Cabral et al. (2020), who evaluated the spatial homogeneity based on two statistics over Germany and found the extremal spatial dependence structure of precipitation is stronger during winter than summer.

All of the GCM-RCM combinations are capable of reproducing the weakening dependence as the distance increases. To quantify the simulation capabilities, we compute the RMSE, as shown in Table 4. In summer, 5 climate model simulations overlap well with the observations and show lower RMSEs, which are MPIESM-RACMO22E, NorESM1-RACMO22E, HadGEM2-HadREM3, HadGEM2-RCA4 and CM5-ALARO-0 simulations. All the five simulations show the same RMSEs of 0.04 (see Table 4). Among the remaining 5 climate model simulations, MPIESM-REMO2009, NoreSM1-REMO2015 and CM5A-REMO2015 significantly underestimate the spatial dependence when the distance between the two grid points are shorter than 200 km. This might be related to the weak spatial dependence of convective precipitation. The MPI-RCA4 and NorESM1-RCA4 simulations significantly overestimate the dependence regardless of the distance.

In winter, the GCM-RCM combinations perform even worse in simulating the spatial dependence. Most of them (8 out of 10) significantly underestimate the spatial dependence (see Figure 2). In particular, MPI-REMO2009, HadGEM2-HadREM3 and CM5A-REMO2015 show systematically a lower spatial dependence regardless of the distance. Other models have a better extremal coefficient behaviour when the distances are small, but a large deviation when two grid points are more than 150 km apart (MPIESM-RACMO22E, NorESM1-REMO2015, NorESM1-RCA4, HadGEM2-RCA4 and CM5-ALARO-0). Only NorESM-RAMCO22E presents the best spatial dependence of extremes in both seasons, as quantified by the RMSE shown in Table 4. The mean RMSE of the ten simulations is 0.102 in winter, while the mean RMSE is 0.072 in

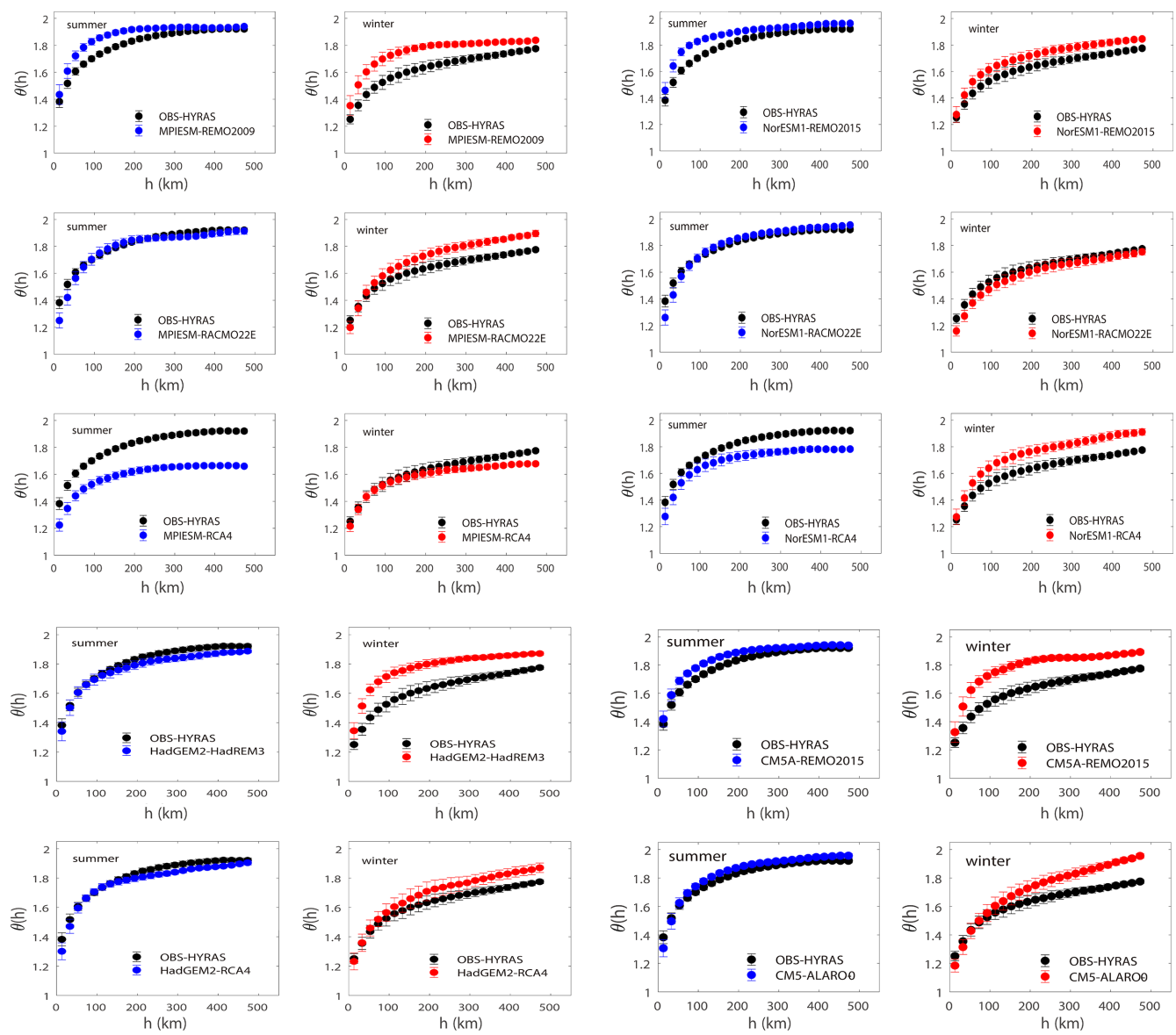


**FIGURE 2** The distribution of the extremal coefficients as a function of pairwise distances in observations (black circles) and climate model simulations (blue circles for summer, red circles for winter). Error bars correspond to one standard deviation. [Colour figure can be viewed at [wileyonlinelibrary.com](http://wileyonlinelibrary.com)]

summer, indicating the spatial dependence of extreme precipitation is worse simulated in winter than in summer. Since GCM-RCM combination outputs are widely used as inputs for the hydrological models to estimate the risk of flooding and study the water resource management, the ability of them in accurately modelling the spatial dependencies is necessary. For example, an underestimation of spatial dependence will lead to a underestimation of the affected area and the probability of joint extreme events. However, our results show that the GCM-RCM combinations lack the ability to well represent the spatial dependencies of extreme precipitation, especially in winter.

Both good GCMs and RCMs are necessary to obtain higher capabilities in simulating the spatial dependence.

Taking the three RCMs driven by the same NorESM1 model as an example, the NorESM1-REMO2015 simulation underestimate the spatial dependence of extremes in summer, while the NorESM1-RCA4 simulation overestimate the dependence. Moreover, if the same RCM is driven by different GCMs, the results will also be different, such as the MPIESM-RCA4, NorESM1-RCA4 and HadGEM2-RCA4 simulations. The first two simulations overestimate the extremal dependence in summer, while the last simulation shows an overall agreement with the observations. Both the quality of GCM and RCM will influence the simulation in reproducing the spatial dependence of extremes. As discussed in Diaconescu et al. (2007) that if large scale-errors are present in the

Season	R1	R2	R3	R4	R5	R6	R7	R8	R9	R10	S
Summer	0.06	<b>0.04</b>	0.22	0.08	<b>0.04</b>	0.11	<b>0.04</b>	<b>0.04</b>	0.05	<b>0.04</b>	<b>0.02</b>
Winter	0.13	0.10	0.05	0.08	<b>0.04</b>	0.12	0.15	0.07	0.16	0.12	<b>0.04</b>

Note: R1:MPIESM-REMO2009, R2:MPIESM-RACMO22E, R3:MPIESM-RCA4, R4:NorESM1-REMO2015, R5:NorESM1-RACMO22E, R6:NorESM1-RCA4, R7:HadGEM2-HadREM3, R8:HadGEM2-RCA4, R9:CM5A-REMO2015, R10:CM5A-ALARO-0. S denotes statistical model (Max-stable model).

TABLE 4 Root-mean-squared-error (RMSE) of different models in presenting the spatial dependence coefficient. The best two models are marked in bold.)

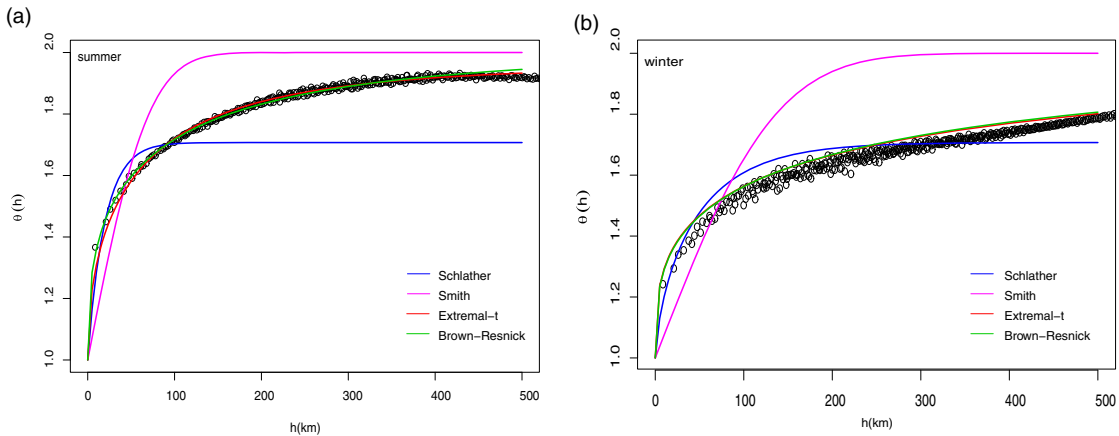


FIGURE 3 The distribution of the extremal coefficient as a function of pairwise distances in observations (black circles) and the fitted extremal coefficient functions (lines) in (a) summer and (b) winter. [Colour figure can be viewed at [wileyonlinelibrary.com](http://wileyonlinelibrary.com)]

Season	Schlather	Smith	Extremal-t	Brown-Resnick
Summer	9,829,916	9,789,065	<b>9,761,672</b>	9,762,466
Winter	9,454,427	9,521,484	<b>9,429,685</b>	9,429,874

Note: Bold font indicates the most parsimonious model.

lateral boundary conditions provided by the GCM, the features in their RCMs will be rather poor. Nevertheless, further studies are needed in how to improve the simulation ability of spatial dependence in GCM-RCM simulations and what mechanisms can account for this behaviour.

The statistical model may overcome the shortcomings of GCM-RCM combinations on simulating the spatial extremes. Figure 3 compares the distribution of the extremal coefficients between the observations and the four fitted max-stable models. In both seasons, the Extremal-t and Brown-Resnick model simulate the spatial dependence well. The Smith model shows that the extremes reach independence at around 120 km in summer and 220 km in winter, which are much earlier than for the observations. The Schlather model cannot well reproduce the dependence at longer distances either. To quantitatively compare the simulation ability, Table 5 shows the goodness of fit quantified by TIC values. The minimum TIC is reached by the Extremal-t model in both seasons, so that we adopt the Extremal-t model to characterize the

TABLE 5 TIC values of different statistical models.

spatial dependence for the statistical model. Compared with the GCM-RCM simulations, the statistical model constructed by the Extremal-t model can better reproduce the observed spatial dependence of extreme precipitation, with the lowest RMSE in both summer and winter.

### 4.3 | Return level of extreme precipitation

The return levels of the statistical model is dependent on both the spatial dependence model and the marginal distribution models. According to the methodology, after we select the appropriate model for the spatial dependence, we need to decide on the marginal distribution of the statistical models. The marginal distributions of the statistical model are modelled by a spatial GEV distribution (Equation 3). The location parameter of the GEV distribution provides the mean intensity of the extremes, while the scale and shape parameters describe how the extremes decay.

According to Equation (3), each parameter of the spatial GEV distribution ( $\mu$ ,  $\sigma$ ,  $\xi$ ) has  $2^3=8$  combinations of covariates (Take  $\mu(x, T)$  in Equation (3) as an example, the 8 combinations are:  $\mu(x, T)=\beta_0^0$ ;  $\mu(x, T)=\beta_0^0+\beta_1^0 \text{lon}(x)$ ;  $\mu(x, T)=\beta_0^0+\beta_2^0 \text{lat}(x)$ ;  $\mu(x, T)=\beta_0^0+\beta_3^0 T$ ;  $\mu(x, T)=\beta_0^0+\beta_1^0 \text{lon}(x)+\beta_2^0 \text{lat}(x)$ ;  $\mu(x, T)=\beta_0^0+\beta_1^0 \text{lon}(x)+\beta_3^0 T$ ;  $\mu(x, T)=\beta_0^0+\beta_2^0 \text{lat}(x)+\beta_3^0 T$ ;  $\mu(x, T)=\beta_0^0+\beta_1^0 \text{lon}(x)+\beta_2^0 \text{lat}(x)+\beta_3^0 T$ ). For the three parameters, there are  $8^3=512$  covariate combinations in total ( $\beta_0^0$ ,  $\beta_1^0$ ,  $\beta_2^0$  must be included). We fit the observed extreme precipitation series to each combination using the maximum-likelihood method, and select the model with the minimum TIC value. The best marginal distributions of the statistical model are shown in Equation (10) for summer

$$\begin{aligned}\mu &\sim \text{lon} + \text{lat} \\ \sigma &\sim \text{lon} + \text{lat} \\ \xi &\sim \text{lon} + \text{lat}\end{aligned}\quad (10)$$

and Equation (11) for winter

$$\begin{aligned}\mu &\sim \text{lon} + \text{lat} + T \\ \sigma &\sim \text{lon} + \text{lat} + T \\ \xi &\sim \text{lon} + T\end{aligned}\quad (11)$$

Different from the marginal models covering the Brandenburg-Berlin region, in which the parameter only consists of longitude or latitude, the models covering the whole of Germany are more complicated (Yang, Franzke, & Fu, 2020a). Both the longitude and latitude are needed to construct the marginal distribution. This is reasonable since we are now dealing with a larger and more spatially complex area which is correspondingly displayed in the complexity of the statistical model.

The best marginal model in summer does not consist of temperature covariate, which indicates that the temperature does not show a significant impact with the historical extreme precipitation in summer. The marginal distribution in winter including temperature as the covariate shows the minimum TIC value, indicating that global warming has a significant influence on the extreme precipitation magnitudes in winter. The findings that there are significant positive trends of extreme precipitation during the winter season, but insignificant overall trends in the summer season in Germany, are consistent with previous studies (Moberg & Jones, 2005; Tabari et al., 2020). The changes of extreme precipitation anomalies are modulated by both large atmospheric circulations and anthropogenic activities (Chen & Sun, 2021; Tabari & Willems, 2018; Xu et al., 2021). By comparing ALL and GHG-alone forcing

CMIP6 simulations, Tabari et al. (2020) found that the contributions of anthropogenic influences to extreme precipitation is latitude dependent and can reach up to 26%–41% for latitudes between 50° and 60°. The contributions are also seasonally dependent, with a weaker contribution in summer and a more robust signal in winter.

Figure 4 shows the geographical distribution of the 25-year return level estimated from observations and the difference with the GCM-RCM combinations and the statistical model in summer. The observed 25-year return levels ranges from 50 mm to 80 mm for most regions of Germany in summer. High intensities of more than 100 mm are mostly observed in the regions of the Bavarian Alps along the southern boundary of Germany, which might be associated with the advection of moist warm air from the Mediterranean basin (Murawski et al., 2016). Most models show large dry biases in the southern and eastern parts of Germany and wet biases in the western part. The results are consistent with Prein et al. (2016), who also find the underestimation of simulated extreme precipitation in the Southeastern Germany and overestimation in Central and Western Germany by the use of eight simulations from the EURO-CORDEX ensemble. It is notable that in contrast to other models, NorESM1-RACMO22E and HadGEM2-HadREM3 exhibit large dry biases; while MPIESM-REMO2009 and CNRM-CM5-ALARO-0 show large wet biases over most of the regions. In HadGEM2-HadREM3, the large dry bias is more than 50 mm, mostly located in southern and eastern Germany.

Table 6 shows the RMSEs of the 25-year return levels simulated by the 10 GCM-RCM simulations and the statistical model. The MPIESM-RACMO22E and the statistical model show the best performance in reproducing the 25-year return levels in summer. The RMSEs of MPIESM-RACMO22E and the statistical model are 10.20 mm (percentage of RMSE [pRMSE]: 17.64%) and 11.26 mm [pRMSE:19.48%]), respectively. The percentages of the RMSE values are calculated since the differences in the absolute RMSE values are not obvious. The HadGEM2-HadREM3 is the worst, the RMSE of which is almost twice of the best model. The statistical model is able to well present the magnitudes of observed extreme precipitation in summer, though it shows an obvious overestimation of return levels in the south-eastern part of Germany.

In winter, the 25-year return levels range from 20 to 40 mm over most of the regions (see Figure 4). High intensities of more than 60 mm are located in the south of Nordrhein-Westfalen, north of Baden-Württemberg and east of Bavaria. The spatial patterns of the return levels in winter are strongly affected by orography. Most of the high-return levels are located in mountainous

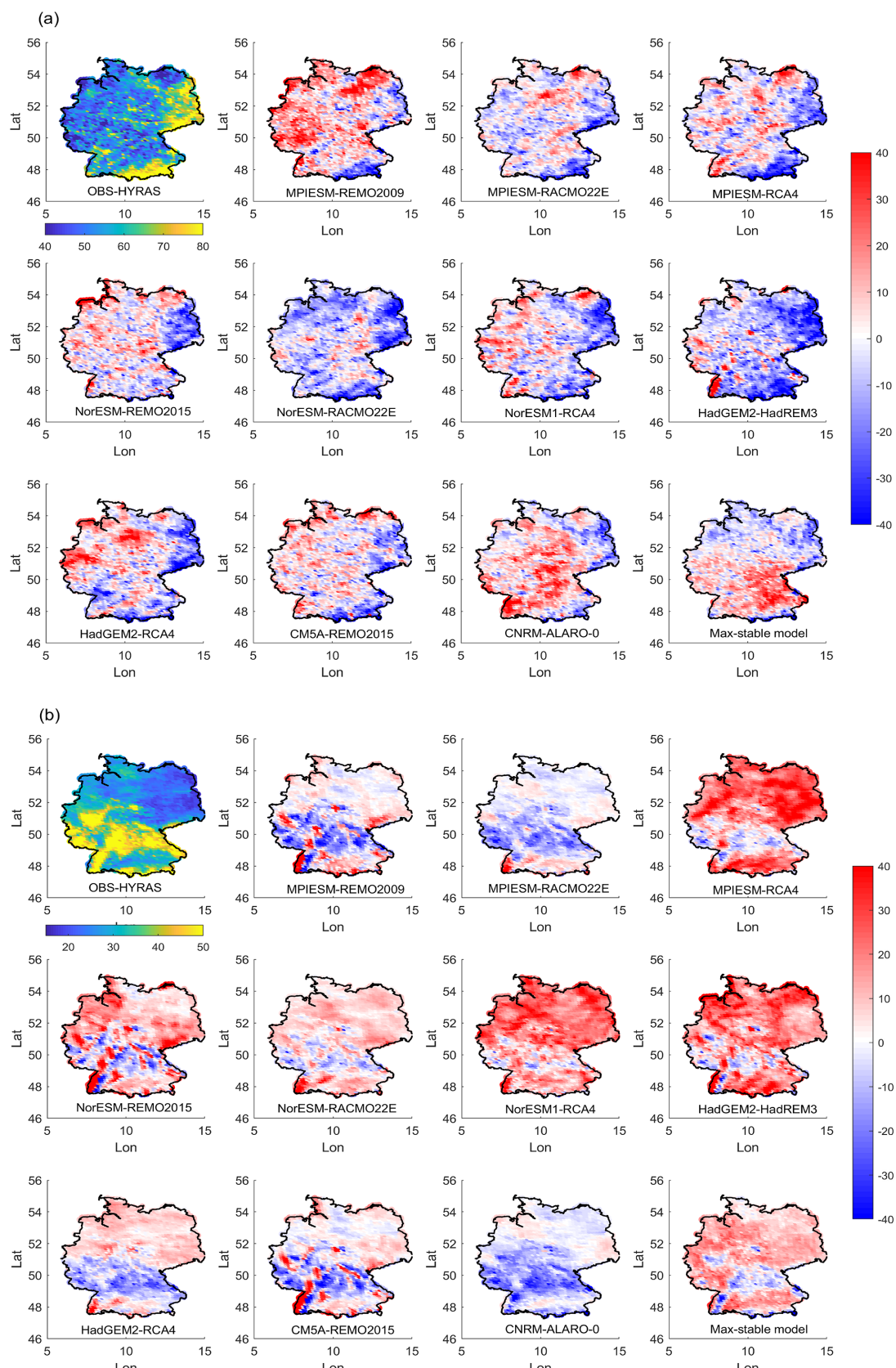


**FIGURE 4** Geographical distributions of intensity (mm) at 25-year return levels of observation, and absolute bias from simulations of global climate model-regional climate model (GCM-RCM) combinations and Max-stable model in (a) summer and (b) winter. [Colour figure can be viewed at [wileyonlinelibrary.com](http://wileyonlinelibrary.com)]

**TABLE 6** Root-mean-squared-error (RMSE) (unit: mm) of different models in presenting the 25-year return levels (the best two models are marked in bold.)

Season	R1	R2	R3	R4	R5	R6	R7	R8	R9	R10	S
Summer	12.38	<b>10.20</b>	12.62	11.52	12.78	12.49	16.21	13.64	<b>11.26</b>	12.53	<b>11.26</b>
Winter	11.16	<b>7.35</b>	20.44	15.14	<b>8.64</b>	18.19	19.24	9.06	11.32	8.77	11.64

Note: R1:MPIESM-REMO2009, R2:MPIESM-RACMO22E, R3:MPIESM-RCA4, R4:NorESM1-REMO2015, R5:NorESM1-RACMO22E, R6:NorESM1-RCA4, R7:HadGEM2-HadREM3, R8:HadGEM2-RCA4, R9:CM5A-REMO2015, R10:CM5A-ALARO-0. S denotes statistical model (Max-stable model).

regions. The mountainous regions, by having complex orography interacting with atmospheric flows, modulate the extreme precipitation. Most simulations show an underestimation in the south and an overestimation in the north. The bias of the model simulations is largely dependent on the downscaling models. The simulations downscaled by REMO2015 and REMO2009 have strongly shifted patterns over the main orographic features of Germany. The simulations downscaled by RCA4 show positive biases in the northern and southern boundaries, but negative biases in the central part. Among the 10 simulations, the best two models are MPIESM-RACMO22E and NorESM1-RACMO22E, with the RMSE values of 7.35 mm (pRMSE:21.33%) and 8.64 mm (pRMSE:25.07%) (see Table 6). The worst model is MPIESM-RCA4, with RMSE value of 20.44 mm (pRMSE:59.32%). The models of MPIESM-RACMO22E and MPIESM-RCA4, which has the same GCM but different RCM, perform totally different in the capabilities in simulating the extreme precipitation, as one being the best while the other is the worst. It indicates that the selection of the RCM has an important impact on the extreme precipitation intensity. In comparison with the other GCM-RCM combinations (such as the NorESM1-REMO2015 and NorESM1-RACMO22E), similar results can be obtained. The results that the RCMs play a dominant role in biases of extreme precipitation intensity simulation over Europe are consistent with previous studies (Berg, Wagner, et al., 2013; Vautard et al., 2021). The dependence may probably be due to the physical parameterizations in the RCMs. The statistical model also lacks the ability to well represent the orographic feature. It underestimates the intensities over the mountains and overestimates the intensities in other areas. The statistical model is ranked the seventh of all the 11 models, as it cannot well reproduce the localized high intensities.

Overall, there is large spread in simulating the 25-year return level in the GCM-RCM combination ensembles in both summer and winter. If we take an average of RMSE of the 10 simulations, it presents a lower RMSE of 12.56 mm (pRMSE: 21.72%) in summer, compared with the 12.93 mm (pRMSE: 37.52%) in winter, indicating that the 0.11° EURO-CORDEX simulations perform better in reproducing the extreme precipitation intensities in summer than in winter. Many previous studies have also

evaluated the dynamical climate models on simulating the extreme precipitation and attempted to explain the reasons for the bad performances. A few studies have found that the climate model simulations produces stronger biases of precipitation in winter than in summer in Germany (Berg, Moseley, & Haerter, 2013a; Toelle et al., 2018; Vautard et al., 2021). By using the nine ensemble RCMs, Rauscher et al. (2009) found that the ensemble mean presents a 20% bias of amount in precipitation in winter and less than 10% bias in summer over Europe. The seasonal difference may be attributed to the seasonal dependence of the gauge undercatch in the observations, which tend to be larger in winter than in summer (Rauscher et al., 2009; Tian et al., 2007; Yang et al., 2005).

In summary, we evaluated how well the 10 GCM-RCM combinations simulate extreme precipitation with respect to temporal clustering, spatial dependence of extremes and intensities during the period 1961–2005 over Germany. Most GCM-RCM combinations produce more serially and spatially independent extreme precipitation events in winter, and some GCM-RCM combinations, such as NorESM1-RCA4 and MPIESM-RCA4 significantly overestimate the spatial dependencies of extremes in summer. The max-stable statistical model, constructed by the Extremal-t function, can relatively well reproduce the spatial dependence. The intensity of the extremes simulated by the max-stable ranked the second in summer and seventh in winter among the 11 climate simulations.

## 5 | FUTURE PROJECTIONS

While observations tell us about the present-day situation of extreme precipitation events, climate models enable us to study the characteristics of projected future extreme precipitation and their likely future change. Though previous studies have demonstrated that climate change will have a significant impact on the magnitude and frequency of extreme precipitation (Wagner et al., 2013), how climate change will affect the temporal and spatial dependencies of extreme precipitation has not been widely addressed so far. A better understanding of how the temporal and spatial dependencies of extreme precipitation will change in a warmer climate is important for

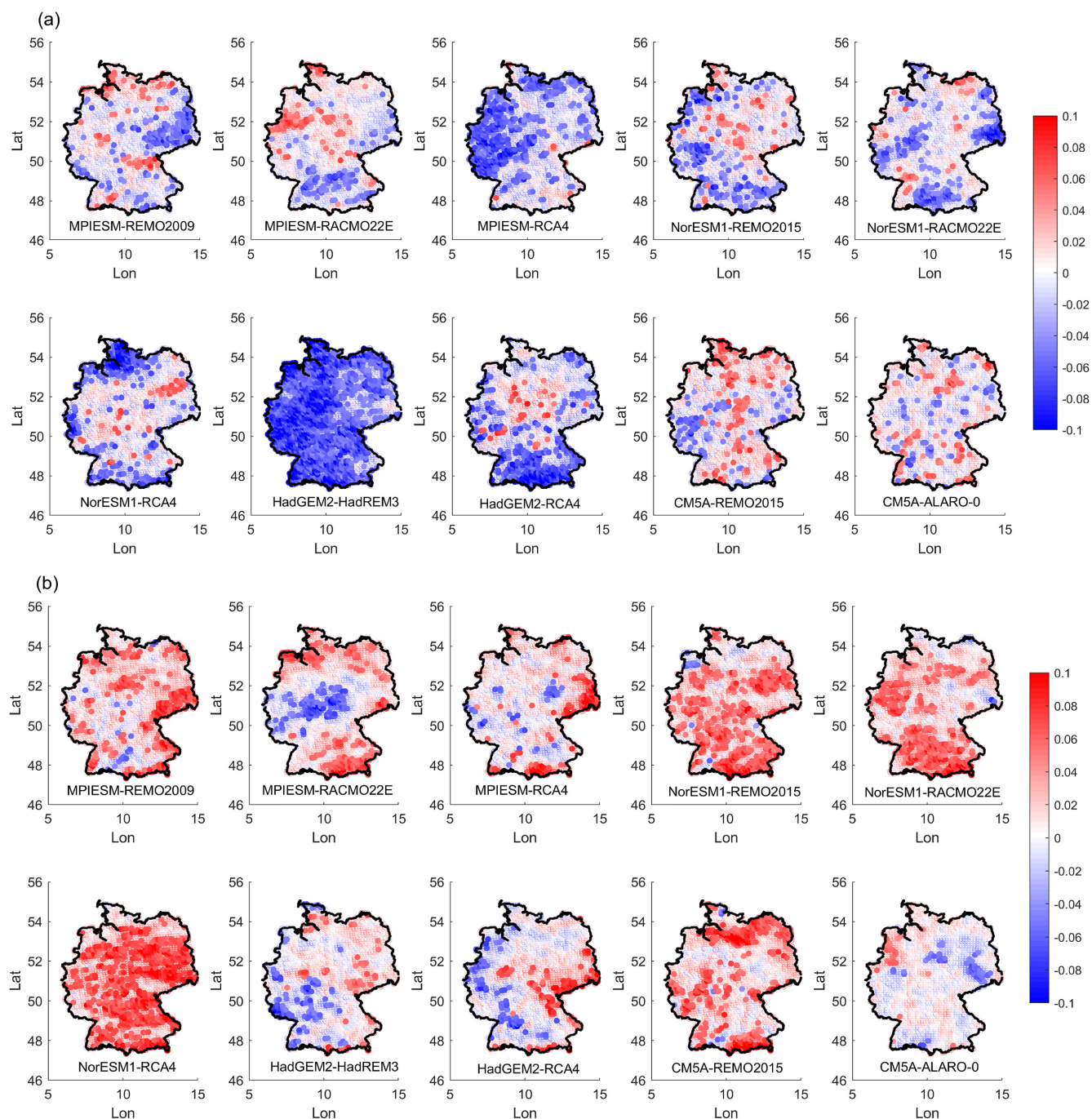


**FIGURE 5** Geographical distributions of the extremal index changes of projected extreme precipitation under RCP8.5 during the period 2056 through 2100 relative to the period of 1961 through 2005 in (a) summer and (b) winter. The filled circles mean the differences have passed 95% significant tests. [Colour figure can be viewed at [wileyonlinelibrary.com](http://wileyonlinelibrary.com)]

many climate impact studies, especially impact studies investigating the likely future changes of natural hazards. Spatial extremes are important for estimating the projected probability of joint extreme events and water resource management. Since our max-stable model has regional temperature as a co-variate in winter, we can also obtain a projected statistical extreme precipitation model in winter with the projected temperature taken from the GCM-RCM combinations.

### 5.1 | Temporal dependence of extreme precipitation

We find that climate change will have a significant impact on the temporal dependencies of extreme precipitation. Figure 5 shows the geographical distributions of the extremal index changes of projected extreme precipitation under RCP8.5 during the period 2056 through 2100 relative to the period of 1961 through 2005. In the

TABLE 7 The mean change of extremal index averaged over Germany.

Season	R1	R2	R3	R4	R5	R6	R7	R8	R9	R10	Mean
Summer (rcp2.6)	0.012	0.006	-0.047	-0.022	0.008	0.006	-0.056	-0.026	0.026	0.014	-0.008
Summer (rcp8.5)	-0.021	0.001	-0.061	-0.033	-0.045	-0.052	-0.071	-0.059	0.015	0.012	-0.031
Winter (rcp2.6)	0.042	0.023	0.042	0.045	0.061	0.072	-0.018	-0.057	0.021	0.048	0.028
Winter (rcp8.5)	0.059	0.020	0.051	0.063	0.064	0.075	-0.017	0.016	0.071	-0.016	0.039

Note: R1:MPIESM-REMO2009, R2:MPIESM-RACMO22E, R3:MPIESM-RCA4, R4:NorESM1-REMO2015, R5:NorESM1-RACMO22E, R6:NorESM1-RCA4, R7:HadGEM2-HadREM3, R8:HadGEM2-RCA4, R9:CM5A-REMO2015, R10:CM5A-ALARO-0.

summer season, more significant decreases of extremal indices can be found among the GCM-RCM simulations, which indicate that the extremes will be more clustered. In particular, the MPIESM-RCA4 and HadGEM2-HadREM3 simulations show more clustered extremes almost across the whole of Germany. The mean change of extremal index averaged over Germany in each simulation is summarized in Table 7. Seven out of 10 simulations show a lower mean change of extremal index under the RCP8.5 scenario, indicating that the extremes under RCP8.5 will be more clustered. While under the RCP2.6 scenario, four simulations show more clustered extremes while the other simulations show more independent extremes.

In winter, the changes of extreme precipitation are totally different from the results in summer. More GCM-RCM combinations show higher extremal index values under the RCP8.5 scenario (see Figure 5), indicating that there are more independent extremes. Five GCM-RCM combinations (MPIESM-REMO2009, NorESM1-REMO2015, NorESM1-RACMO22E, NorESM1-RCA4 and CM5A-REMO2015) show there are more independent extremes over Germany, while 3 GCM-RCM combinations (MPIESM-RACMO22E, HadGEM2-HadREM3 and HadGEM2-RCA4) show there are more dependent extremes in Western Germany and more independent extremes in Eastern Germany. The geographical distributions of the changes of the extremal indices under RCP2.6 are similar with those under RCP8.5, but with fewer significant grid points. If we take an average of the changes in the 10 climate simulations over the domain, more temporal clustered extremes in summer and more independent extremes in winter will be projected. And the clustering or independence of the extreme will intensify under high concentration pathways.

## 5.2 | Spatial dependence of extreme precipitation

Figure 6 shows the changes of the extremal coefficients under climate change for the two seasons. In summer, 7 out of 10 GCM-RCM combinations show there are no

significant differences of the spatial dependence of projected precipitation relative to historical conditions. NorESM1-RACMO22E, which is the best model to reproduce the spatial dependence of observed precipitation, shows significantly stronger dependence at large distances under RCP8.5. That means that the magnitudes of the extremes at long distances are strongly correlated and that the extreme events might be more homogeneous. However, the NorESM1-RCA4 and MPIESM-RCA4 show that the extreme magnitudes are significantly less correlated at distances longer than around 100 km under high emission scenarios.

In winter, the result of NorESM1-RACMO22E shows that there is a significant trend of increasing independence under RCP2.6 relative to historical conditions. This indicates that the magnitudes of extremes in winter at different grid points are less correlated, which is a potential sign that the extremes in winter become more localized in the future.

No significant changes of spatial dependences of projected extreme precipitation are found in most GCM-RCM combinations in both summer and winter. One possible reason is that most GCM-RCM combinations lack the ability of well reproducing the spatial dependence of the extremes. A large bias exists between the GCM-RCM combinations and the observation (Figure 2), so that the changes of spatial dependence might not be robust. Further studies are needed in how to improve the simulation ability of spatial dependence and what mechanisms can account for this behaviour.

## 5.3 | Return level of extreme precipitation

The box plot of the relative change of the 25-year return levels in each grid during the period 2056–2100 with respect to the period 1961–2005 under RCP2.6 and RCP8.5 over Germany is shown in Figure 7. Comparisons between the 10 GCM-RCM combinations reveal great agreements in the increasing median values of extreme precipitation intensities in summer. There is a much

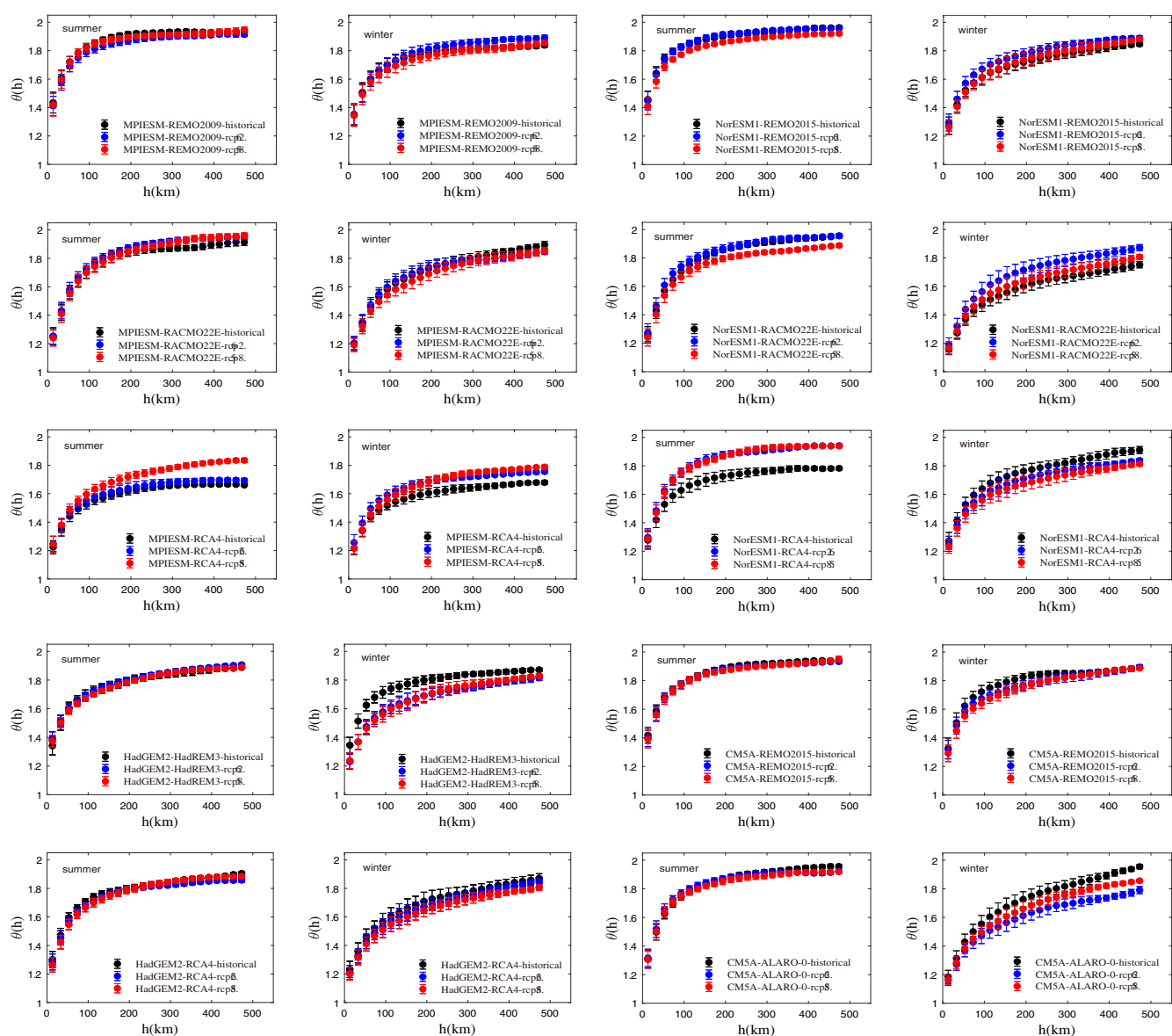


**FIGURE 6** The distribution of the extremal coefficients as a function of pairwise distances in climate model simulations during the period through 1961 to 2005 under historical conditions (black circles), the period through 2056 to 2100 under RCP2.6 scenario (blue circles) and RCP8.5 scenario (red circles). Error bars correspond to one standard deviation. [Colour figure can be viewed at [wileyonlinelibrary.com](http://wileyonlinelibrary.com)]

stronger increase under RCP8.5 than RCP2.6. The mean intensification averaged over all the grid points of extreme precipitation in 10 GCM-RCM combinations ranges from 1.74% (MPIESM-RCA4) to 39.88% (NorESM1-RCA4) under RCP2.6 and from 5.33% (MPIESM-RCA4) to 53.24% (NorESM1-RCA4) under RCP8.5 in summer. All the 10 GCM-RCM combinations simulate that in some regions the increase of the intensities is more than 100%. The multi-model mean shows the 25-year return levels will increase 19.05% under RCP2.6 and 31.41% under RCP8.5. For the investigation of regions which are projected to be more affected by extreme precipitation events in the future, the spatial distributions of the relative changes of 25-year return levels under RCP8.5 are shown in Figure 8.

The multi-model mean presents an overall intensification of extreme precipitation across Germany. For individual GCM-RCM combinations, the projected climate signal is not clear. Apart from MPIESM-RCA4, the other models present positive trends of intensities over most grid points. The projected percentages of wet days of extreme precipitation will also increase in the future period, as shown by Wagner et al. (2013). This indicates that extreme precipitation events not only intensify, but also occur more frequently. The spatial distribution of the projected percentage of wet days is heterogeneous for individual GCM-RCM combination as well. For the statistical modelling in the historical condition, the model in summer does not include the temperature covariance, which indicates that

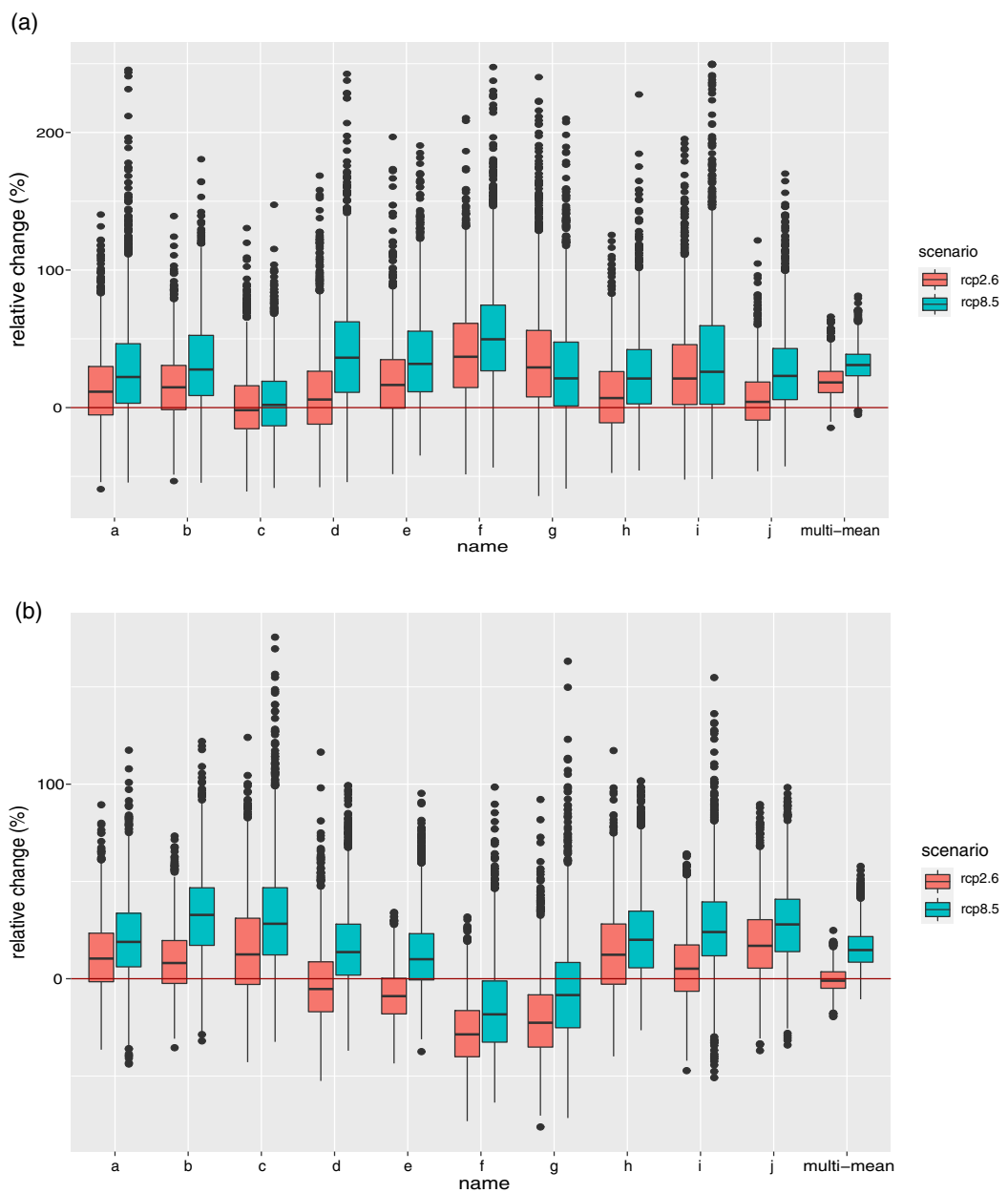


**FIGURE 7** Box plots (median, 25%–75% range and outlier values) of relative intensity changes (%) at 25-year return level in each grid point of Germany for climate model simulations in (a) summer and (b) winter. ('a' stands for 'MPIESM-REMO2009', 'b' stands for 'MPIESM-RACMO22E', 'c' stands for 'MPIESM-RCA4', 'd' stands for 'NorESM1-REMO2015', 'e' stands for 'NorESM1-RACMO22E', 'f' stands for 'NorESM1-RCA4', 'g' stands for 'HadGEM2-HadREM3', 'h' stands for 'HadGEM2-RCA4', 'i' stands for 'CM5A-REMO2015', 'j' stands for 'CM5A-ALARO-0'.) [Colour figure can be viewed at [wileyonlinelibrary.com](http://wileyonlinelibrary.com)]

the warmer climate will not have an impact on the historical extreme precipitation. An assumption is made here that the statistical model that performs well in reproducing past climates is also more likely to yield robust projections for the future. So there are no significant changes of projected extreme precipitation intensity in the statistical model in summer.

In winter, 6 out of 10 GCM-RCM combinations show an increased median intensity under RCP2.6 and 8 out of 10 GCM-RCM combinations show intensification under

RCP8.5 (see Figure 7). The mean increase of extreme precipitation intensities ranges from -27.77% (NorESM1-RCA4) to 18.77% (CM5A-ALARO-0) under RCP2.6 and from -15.38% (NorESM1-RCA4) to 32.23% (MPIESM-RACMO22E) under RCP8.5. The NorESM1-RCA4 and HadGEM2-HadREM3 models show pronounced decreased intensities, especially in the northern part of Germany. For the multi-model mean the extreme intensity is projected to decrease by 0.52% under RCP2.6 and increase by 15.53% under RCP8.5. The increase is more

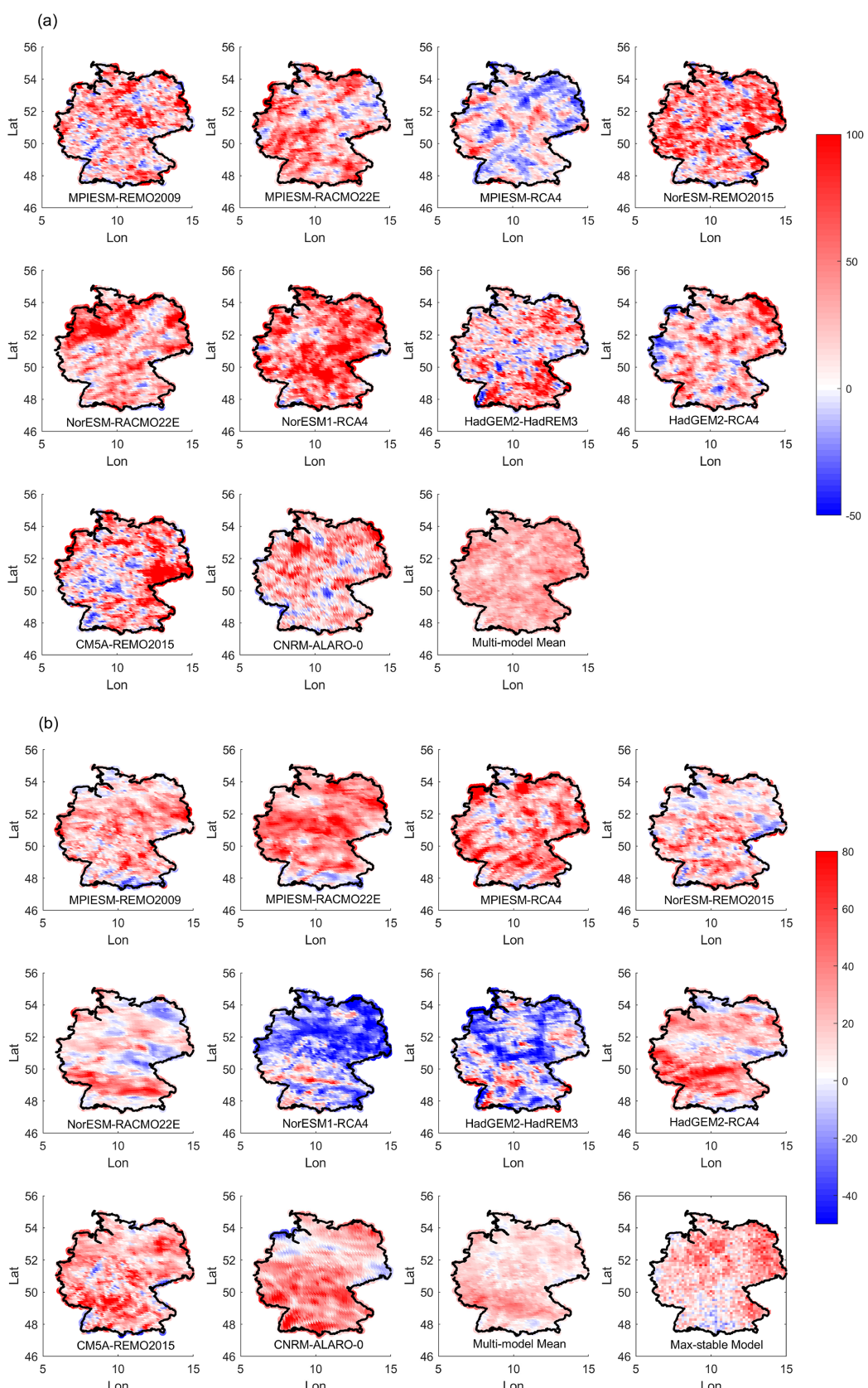


**FIGURE 8** Geographical distributions of the relative 25-year return level changes (%) of the climate model simulations and one statistical model during the period of 2056–2100 (RCP8.5 scenario) relative to the period of 1961–2005 (historical condition) in (a) summer and (b) winter. [Colour figure can be viewed at [wileyonlinelibrary.com](http://wileyonlinelibrary.com)]

likely to occur in South Germany (see Figure 8). The projected max-stable model in winter is generated by the spatial dependence information of the projected NorESM-RACMO22E model and the mean projected temperature of the 10 GCM-RCM combinations. It shows that the intensification of extreme precipitation magnitudes over Germany is 3.02% under RCP2.6 and 4.16% under RCP8.5.

Our statistical future projections are generated under the assumption that the marginal distribution models of extreme precipitation in the historical period is the same as in the future scenarios. However, due to the complex variabilities of the climate system, the marginal distribution models may change under different future scenarios, which increases the uncertainties of the statistical projections. Nevertheless, this is our first attempt to provide a statistical projected extreme precipitation model and it may serve as a complement for climate change studies.

## 6 | CONCLUSIONS AND DISCUSSIONS

The extremes of hydrological variables exhibit substantial dependencies over a wide range of temporal and spatial scales. While most of the extreme precipitation evaluation studies focus on how the models simulate the frequencies or magnitudes of extreme precipitation events, little interest has been paid to the dependencies of the extremes. The temporal dependencies of extremes determine how much the extremes are clustered, which is considered as the main factor to trigger the natural hazards such as flooding. The spatial dependencies of the extremes at two close sites determine the risk that the extremes occur simultaneously. Even if the two sites are further apart, the qualification of the spatial dependence will also help estimate the probabilities of concurrent extremes. So the successive and spatially extended extreme precipitation events have great socio-economic consequences and their probabilities should be assessed precisely.

In this study, we use a spatial extremes framework to systematically study the historical and projected temporal and spatial characteristics of extreme precipitation in Germany. We studied the performance of 10 high-resolution GCM-RCM historical simulations in reproducing the temporal dependence (using the extreme index as a measure), spatial dependence (using the extremal coefficient as a measure) and intensities (using 25-year return levels as a measure) against the 1-km gridded observation dataset (HYRAS) over Germany. A statistical model is also derived and evaluated with regard to the spatial dependence and extreme precipitation intensities.

We find that there is large spread in simulating the extreme precipitation among individual GCM-RCM combinations. In summer, though some GCM-RCM combinations underestimate the temporal clustering of extreme precipitation, the multi-model mean could capture the gross features seen in the observations. The spatial dependencies of extreme precipitation in summer can also be simulated well among 5 out of 10 GCM-RCM combinations. While in the winter season, the simulated extremes are more independent and localized compared with the observations. It shows a larger deviation of temporal extremal index and spatial dependence coefficient compared with observations. The result that the GCM-RCM simulation cannot well reproduce the spatial dependence of extremes at longer distance indicates that the GCM-RCM combinations are not good at simulating the homogeneous large-scale precipitation in winter. This may be attributable to inaccurate simulations of large-scale weather systems due to problematic parameterizations in models. In modelling the extreme intensities, the GCM-RCM simulations present wet biases in the west and drier biases in the east in the summer season, which are consistent with the studies by Prein et al. (2016). While in the winter season, most simulations show wetter biases in the north and underestimate the extremes in the south.

The simulation biases are a combination of both GCMs and RCMs arising from a number of sources. The contributions of the GCM versus RCM in the biases depend on the extremal indices. For simulating the temporal cluster in summer, the selection of GCM impacts the sign of the differences between the simulations and observation while the selection of RCMs impacts the geographical details. For simulating the extreme precipitation intensity, the contribution of RCMs to the biases is dominant. The dominant role of RCMs in simulating the extreme precipitation intensities can also be found in previous studies by Vautard et al. (2021) and Berg, Wagner, et al. (2013b). The max-stable statistical model, constructed by the Extremal-t model, can relatively well represent the spatial dependence and return levels of observed extreme precipitation in summer compared with individual GCM-RCM combinations. The ability of the max-stable model in reproducing the 25-year return level ranks as the second best in the summer and as the seventh best in the winter, among the total 11 climate simulations. In modelling the marginal distribution in winter, the max-stable model including the temperature covariate is the best. We then produce statistical future projections by using the mean temperature under RCP2.6 and RCP8.5 as a covariate.

Global warming will have a significant impact on the temporal clustering and spatial dependence of extreme

precipitation over Germany. Although different GCM-RCM simulations present a different geographical distribution of the temporal extremal index, a relatively general conclusion can be obtained that extremes tend to be more dependent in the summer and more independent in the winter under the RCP8.5 scenario. The inverse tendency of the clustering of extreme precipitation is interesting and deserves further study. The clustering trends in the future projections are also region-dependent. With the 25 GCMs participating in CMIP6, Tuel and Martius (2021) found that the clustering trends in future projections under the SSP85 scenario are strong in the tropics, and generally weak in extra-tropics. Actually, the temporal cluster character of heavy precipitation over Europe has been shown to be associated with the large-scale climate modes, such as AO and NAO (Yang & Villarini, 2019). The changes of temporal cluster of projected extreme precipitation may be modulated by the change of atmospheric modes under global warming (Tuel & Martius, 2021). Atmospheric Rivers, which bring air with high water content, also has impacts on the dry/wet pattern of extreme precipitation in Germany, which may have an influence on the temporal cluster of projected extreme precipitation (Lavers & Villarini, 2013; Newell et al., 1992). Besides the temporal dependencies, global warming may also influence the spatial dependencies. The NorESM1-RACMO22E, which could best simulated the observed spatial dependence, shows that the extremes will be more localized in winter and more homogeneous in summer under RCP8.5.

Although few studies have considered the changes of spatial dependence of extreme precipitation, some studies examined the changes in the size of geographical area impacted by extreme precipitation events. The size of the affected geographical area by extreme precipitation events is associated with the spatial dependence of the extremes, since a higher spatial dependence of the extreme values at two close gridpoints may indicate a higher probability of extremal concurrence. However, among those studies, how the size of the affected area changes with a warmer climate is still under debate. Prein et al. (2017) and Berg, Moseley, and Haerter (2013) found that the spatially extended precipitation event size is increasing with the global warming. On the other hand, Wasko et al. (2016) showed that the spatial extent of extreme precipitation events decrease with warmer temperature in Australia. Benestad (2018) suggested the spatial extent of daily precipitation episodes has decreased in the last decade leading to more intense localized precipitation. Moreover, climate projections show a considerable decrease of spatial extent of up to 28% by the end of the century. Recently, Matte et al. (2022) investigated the adjacent areas affected by the 20-year extreme daily precipitation events over Europe by

the use of 19 members from the 0.11° GCM-RCM simulations. Their studies show that the GCM-RCM simulations are able to represent a similar size distribution of the area affected by extreme precipitation events, compared with the reanalysis ERA5. And the size distribution of extreme precipitation events in the European case is due to the RCM physical parametrizations. Under the global warming, the affected area will become larger for all of Europe as well as various sub-regions.

The climatic change also has an impact on the magnitudes of extreme precipitation, but a large spread exists between models. As pointed out by Araujo et al. (2022), the changes of extreme precipitation under global warming are dependent on the locations, timescales and percentiles. In our study, the 10 high-resolution GCM-RCM combinations all show an intensification of the mean extreme precipitation averaged over Germany quantified by 25-year return levels in summer. The multi-model mean shows the 25-year return levels will increase by 19.05% under RCP2.6 and 31.41% under RCP8.5. Among each simulation, the mean relative intensification averaged over all the grid points ranges from 1.74% to 39.88% under RCP2.6 and from 5.33% to 53.24% under RCP8.5. In some regions, the intensification is more than 100%. In winter, the ensemble mean shows a decrease of 0.52% under RCP2.6 and an increase of 15.53% under RCP8.5. In particular, NorESM1-RCA4 and HadGEM2-HadREM3 show decrease of extreme precipitation under the two scenarios, while the NorESM1-REMO2015 and NorESM1-RACMO22E show decreased extreme precipitation under RCP2.6. The other GCM-RCM combinations present intensification with the mean relative increase ranging from 5.55% to 18.77% under RCP2.6 and from 12.92% to 32.23% under RCP8.5. The statistical model projections also show that the extreme precipitation will be heavier in winter due to global warming, with the mean increase of 3.02% under RCP2.6 and 4.16% under RCP8.5.

It is widely accepted that an increase of heavy precipitation intensity will be projected by most dynamical climate models in the northern and central Europe, but the simulations disagree on the magnitudes and geographical details of the signals (Araujo et al., 2022; Luu et al., 2018; Santos et al., 2019). Wagner et al. (2013) studied the projected heavy precipitation over Germany based on two GCMs (ECHAM5 and CCCma3) and two RCMs (CLM and WRF). A general increase of heavy precipitation intensities can be found, but the changes vary significantly for different ensemble members so that no robust results can be obtained. In the south of France, the intensity of a 1-in-100 year event in the historical climate may increase with an uncertainty of between 1% and 27% by using 10 EURO-CORDEX simulations (Luu et al., 2018).

In some regions, the spread of climate models is comparable or sometimes even larger than the climate change signal (Zittis et al., 2019). By using 22 EURO-CORDEX ensemble simulations, Rajczak and Schar (2017) found that the simulation spread is seemingly larger in summer than winter in central Europe. The RCM ensemble show a spread ranging from 4% to 44% for the changes in the summer 50-year return level and 13% to 39% for the changes in winter during the period 2070–2099 relative to the period 1981–2010. Overall, in the majority seasons and regions of Europe, the heavy precipitation will intensify (Coppola et al., 2020). Different from the extreme temperature, the inter-model agreement and robustness of extreme precipitation projections are much lower. Nowadays, to improve the extreme precipitation simulation capabilities and provide more reliable extreme precipitation projections, many research groups tried to produce convective-permitting climate simulations, which would resolve better convective processes at local scale and interactions with large-scale circulation. It is expected that more detailed structures of extreme precipitation and more similarity to observations will be presented (Luu et al., 2022; Prein et al., 2015). The better simulation generated by the convective-permitting models may provide more reliable climate change studies and its impacts.

## AUTHOR CONTRIBUTIONS

**Lichao Yang:** Conceptualization; investigation; writing – original draft; methodology; validation; visualization; writing – review and editing; formal analysis. **Christian L. E. Franzke:** Conceptualization; investigation; writing – review and editing; methodology; formal analysis. **Wansuo Duan:** Writing – review and editing; supervision.

## ACKNOWLEDGEMENTS

We thank two anonymous reviewers for their comments. The study was sponsored by the National Nature Scientific Foundation of China (grant no. 42105061). Christian L. E. Franzke was supported by the Institute for Basic Science (IBS), Republic of Korea, under IBS-R028-D1, and National Research Fund of Korea (NRF-2022M3K3A1097082). We wish to thank Dr. Mathieu Ribatet for providing the ‘SpatialExtremes’ R package.

## CONFLICT OF INTEREST STATEMENT

The authors declare no conflict of interest.

## ORCID

Lichao Yang  <https://orcid.org/0000-0003-4889-7382>  
 Christian L. E. Franzke  <https://orcid.org/0000-0003-4889-7382>

4111-1228

Wansuo Duan  <https://orcid.org/0000-0002-0122-2794>

## REFERENCES

- Alexander, L.V. & Arblaster, J.M. (2017) Historical and projected trends in temperature and precipitation extremes in Australia in observations and CMIP5. *Weather and Climate Extremes*, 15, 34–56.
- Araujo, J.R., Ramos, A.M., Soares, P.M.M., Melo, R., Oliveria, S. C. & Trigo, R.M. (2022) Impact of extreme rainfall events on landslide activity in Portugal under climate change scenarios. *Landslides*, 19, 2279–2293.
- Barton, Y., Giannakaki, P., Waldow, H.V., Chevalier, C., Pfhal, S. & Martius, O. (2016) Clustering of regional-scale extreme precipitation events in southern Switzerland. *Monthly Weather Review*, 144, 347–369.
- Benestad, R.E. (2018) Implications of a decrease in the precipitation area for the past and the future. *Environmental Research Letters*, 13(4), 044022.
- Berg, P., Moseley, C. & Haerter, J.O. (2013a) Strong increase in convective precipitation in response to higher temperatures. *Nature Geoscience*, 6(3), 181–185.
- Berg, P., Wagner, S., Kunstmann, H. & Schaedler, G. (2013b) High resolution regional climate model simulations for Germany: part I—validation. *Climate Dynamics*, 40, 401–414.
- Bernardara, P., De Michele, C. & Rosso, R. (2007) A simple model of rain in time: an alternating renewal process of wet and dry states with a fractional (non-gaussian) rain intensity. *Atmospheric Research*, 84(4), 291–301.
- Cabral, R., Ferreira, A. & Friederichs, P. (2020) Space–time trends and dependence of precipitation extremes in North-Western Germany. *Environmetrics*, 31(3), e2605.
- Chen, H. & Sun, J. (2021) Anthropogenic influence has increased climate extreme occurrence over China. *Science Bulletin*, 66(8), 749–752.
- Coles, S. (2001) *An introduction to statistical modeling of extreme values*. London, U.K.: Springer-Verlag.
- Cooley, D., Naveau, P. & Poncet, P. (2006) *Dependence in probability and statistics*. New York, NY: Springer.
- Coppola, E., Nogherotto, R., Ciarlo', J.M., Giorgi, F., van Meijgaard, E., Kadygrov, N. et al. (2020) Assessment of the European climate projections as simulated by the large EURO-CORDEX regional and global climate model ensemble. *Journal of Geophysical Research: Atmospheres*, 126(4), e2019JD032356.
- de Haan, L. (1984) A spectral representation for max-stable processes. *The Annals of Probability*, 12(4), 1194–1204.
- de Haan, L. & Pereira, T.T. (2006) Spatial extremes: models for the stationary case. *The Annals of Statistics*, 34(1), 146–168.
- Diaconescu, E.P., Laprise, R. & Sushama, L. (2007) The impact of lateral boundary data errors on the simulated climate of a nested regional climate model. *Climate Dynamics*, 28, 333–350.
- Diaconescu, E.P., Mailhot, A., Brown, R. & Chaumont, D. (2018) Evaluation of CORDEX-Arctic daily precipitation and temperature-based climate indices over Canadian Arctic land areas. *Climate Dynamics*, 50, 2061–2085.
- Donat, M.G., Lowry, A.L., Alexander, L.V., O'Gorman, P.A. & Maher, N. (2016) More extreme precipitation in the world's dry and wet regions. *Nature Climate Change*, 6, 508–513.

- Dosio, A. & Fischer, E.M. (2018) Will half a degree make a difference? Robust projections of indices of mean and extreme climate in Europe under 1.5°C, 2°C, and 3°C global warming. *Geophysical Research Letters*, 45, 935–944.
- Ehmele, F., Kautz, L., Feldmann, H. & Pinto, J.G. (2020) Long-term variance of heavy precipitation across Central Europe using a large ensemble of regional climate model simulations. *Earth System Dynamics*, 11, 469–490.
- Ferreira, M. (2018) Heuristic tools for the estimation of the extremal index: a comparison of methods. *Revstat-Statistical Journal*, 16(1), 115–136.
- Franzke, C.L.E. (2017) Impacts of a changing climate on economic damages and insurance. *Economics of Disaster and Climate Change*, 1(1), 95–110.
- Franzke, C.L.E. (2021) Towards the development of economic damage functions for weather and climate extremes. *Ecological Econ.*, 1989, 1–12.
- Franzke, C.L.E. & Torelló i Sentelles, H. (2020) Risk of extreme high fatalities due to weather and climate hazards and its connection to large-scale climate variability. *Climatic Change*, 162, 141–157.
- Gu, L., Chen, J., Yin, J., Xu, C. & Zhou, J. (2020) Responses of precipitation and runoff to climate warming and implications for future drought changes in China. *Earth's Futures*, 8, e2020EF001718.
- Halleygate, S., Green, C., Nicholls, R.J. & Corfee-Morlot, J. (2013) Future flood losses in major coastal cities. *Nature Climate Change*, 3, 802–806.
- Hannachi, A. (2014) Intermittency, autoregression and censoring: a first-order AR model for daily precipitation. *Meteorological Applications*, 21(2), 384–397.
- Hu, G. & Franzke, C. (2020) Evaluation of daily precipitation extremes in reanalysis and gridded observation based data sets over Germany. *Geophysical Research Letters*, 47, e2020GL089624.
- Jacob, D., Teichmann, C., Sobolowski, S., Katragkou, E., Anders, I., Belda, M. et al. (2020) Regional climate downscaling over Europe: perspectives from the EURO-CORDEX community. *Regional Environmental Changes*, 53, 759–778.
- Kim, D. & Onof, C. (2020) A stochastic rainfall model that can reproduce important rainfall properties across the timescales from several minutes to a decade. *Journal of Hydrology*, 589, 125150.
- Kopp, J., Rivoire, P., Ali, S.M., Barton, Y. & Martius, O. (2021) A novel method to identify sub-seasonal clustering episodes of extreme precipitation events and their contributions to large accumulation periods. *Hydrology and Earth Sciences Discussions*, 67, 5153–5174.
- Laflamme, E.M., Linder, E. & Pan, Y. (2016) Statistical downscaling of regional climate model output to achieve projections of precipitation extremes. *Weather and Climate Extremes*, 12, 15–23.
- Lavers, D.A. & Villarini, G. (2013) The nexus between atmospheric rivers and extreme precipitation across Europe. *Geophysical Research Letters*, 40, 3259–3264.
- Luu, L.N., Vautard, R., Yiou, P. & Souleyroux, J.M. (2022) Evaluation of convection-permitting extreme precipitation simulations for the south of France. *Earth System Dynamics*, 13, 687–702.
- Luu, L.N., Vautard, R., Yiou, P., van Oldenborgh, G.J. & Lenderink, G. (2018) Attribution of extreme rainfall events in the south of France using EURO-CORDEX simulations. *Geophysical Research Letter*, 45, 6242–6250.
- Martius, O., Sodemann, H., Joos, H., Pfahl, S., Winschall, A., Croci-Maspoli, M. et al. (2013) The role of upper-level dynamics and surface processes for the Pakistan flood of July 2010. *Quarterly Journal of the Royal Meteorological Society*, 139, 1780–1797.
- Masson-Delmotte, V., Zhai, P., Pirani, A., Connors, S., Péan, C., Berger, S., Caud, N., Chen, Y., Goldfarb, L., Gomis, M., Huang, M., Leitzell, K., Lonnoy, E., Matthews, J., Maycock, T., Waterfield, T., Yelekçi, O., Yu, R., Zhou, B. (2021). *Climate change 2021: the physical science basis: working group I contribution to the sixth assessment report of the intergovernmental panel on climate change*. Cambridge, UK and New York: Cambridge University Press.
- Matte, D., Christense, J.H. & Ozturk, T. (2022) Spatial extent of precipitation events: when big is getting bigger. *Climate Dynamics*, 58, 1861–1875.
- Merz, B., Kreibich, H., Schwarze, R. & Thielen, A. (2010) Assessment of economic flood damage. *Natural Hazards and Earth System Sciences*, 10(8), 1697–1724.
- Moberg, A. & Jones, P.D. (2005) Trends in indices for extremes in daily temperature and precipitation in central and western Europe, 1901–99. *International Journal of Climatology*, 25(9), 1149–1171.
- Moloney, N.R., Faranda, D. & Sato, Y. (2019) An overview of the extremal index. *Chaos*, 29(2), 022101.
- Murawski, A., Zimmer, J. & Merz, B. (2016) High spatial and temporal organization of changes in precipitation over Germany for 1951–2006. *International Journal of Climatology*, 36(6), 2582–2597.
- Newell, R.E., Newell, N.E., Zhu, Y. & Scott, C. (1992) Tropospheric rivers?—A pilot study. *Geophysical Research Letters*, 19, 2401–2404.
- O'Gorman, P. & Schneider, T. (2009) The physical basis for increases in precipitation extremes in simulations of 21st-century climate change. *Proceedings of the National Academy of Sciences of the United States of America*, 106(35), 14773–14777.
- Paschalidis, A., Molnar, P., Faticchi, S. & Burlando, P. (2013) A stochastic model for high-resolution space-time precipitation simulation. *Water Resources Research*, 49(12), 8400–8417.
- Pendergrass, A.G. & Knutti, R. (2018) The uneven nature of daily precipitation and its change. *Geophysical Research Letters*, 45, 11980–11988.
- Prein, A.F., Gobiet, A., Truhetz, H., Keuler, K., Goergen, K. et al. (2016) Precipitation in the EURO-CORDEX 0.11 and 0.44 simulations: high resolution, high benefits? *Climate Dynamics*, 46, 383–412.
- Prein, A.F., Langhans, W., Fosser, G., Ferrone, A., Ban, N., Goergen, K. et al. (2015) A review on regional convection-permitting climate modeling: demonstrations, prospects, and challenges. *Reviews of Geophysics*, 53, 323–361.
- Prein, A.F., Liu, C., Ikeda, K., Trier, S.B., Rasmussen, R.M., Hollabd, G.J. et al. (2017) Increased rainfall volume from future convective storms in the US. *Nature Climate Change*, 7(12), 880–884.
- Rajczak, J. & Schar, C. (2017) Projections of future precipitation extremes over Europe: a multimodel assessment of climate simulations. *Journal of Geophysical Research: Atmosphere*, 122, 10773–10880.

- Rauscher, S.A., Coppola, E., Piani, C. & Giorgi, F. (2009) Resolution effects on regional climate model simulations of seasonal precipitation over Europe. *Climate Dynamics*, 35, 685–711.
- Rauthe, M., Steiner, H., Riediger, U., Mazurkiewicz, A. & Gratzki, A. (2013) A central European precipitation climatology—part I: generation and validation of a high-resolution gridded dailydata set (HYRAS). *Meteorologische Zeitschrift*, 22(3), 235–256.
- Ribatet, M. (2009) *A user's guide to the SpatialExtremes package*. Lausanne, Switzerland: EPFL.
- Ribatet, M. (2017). Modelling spatial extremes using max-stable processes. Em Franzke, C. L. E. e O'Kane, T., editores, *Non-linear and stochastic climate dynamics*, pgs. 369–391. Cambridge University Press, Cambridge.
- Santos, M., Fonseca, A., Fragoso, M. & Santos, J. (2019) Recent and future changes of precipitation extremes in mainland Portugal. *Theoretical and Applied Climatology*, 137(1–2), 1305–1319.
- Sunyer, M.A., Luchner, J., Onof, C., Madsen, H. & Arnbjerg-Nielsen, K. (2016) Assessing the importance of spatio-temporal RCM resolution when estimating sub-daily extreme precipitation under current and future climate conditions. *International Journal of Climatology*, 37(2), 688–705.
- Tabari, H., Madani, K. & Willems, P. (2020) The contribution of anthropogenic influence to more anomalous extreme precipitation in Europe. *Environmental Research Letters*, 15(10), 104077.
- Tabari, H. & Willems, P. (2018) Lagged influence of Atlantic and Pacific climate patterns on European extreme precipitation. *Scientific Reports*, 8, 5748.
- Tian, X., Dai, A., Yang, D. & Xie, Z. (2007) Effects of precipitation-bias corrections on surface hydrology over northern latitudes. *Journal of Geophysical Research Atmospheres*, 112, D14101.
- Toelle, M.H., Schefczyk, L. & Gutjahr, O. (2018) Scale dependency of regional climate modeling of current and future climate extremes in Germany. *Theoretical and Applied Climatology*, 134, 829–848.
- Tuel, A. & Martius, O. (2021) A global perspective on the sub-seasonal clustering of precipitation extremes. *Weather and Climate Extremes*, 33(20), 100348.
- van der Wiel, K., Kapnick, S.B., Vecchi, G.A., Cooke, W.F., Delworth, T.L., Jia, L. et al. (2016) The resolution dependence of contiguous U.S. precipitation extremes in response to CO<sub>2</sub> forcing. *Journal of Climate*, 29, 7991–8012.
- van Vuuren, D.P., Edmonds, J.A., Kainuma, M., Riahi, K. & Weyant, J. (2011) A special issue on the RCPs. *Climatic Change*, 109(1), 1–4.
- Varin, C. & Vidoni, P. (2005) A note on composite likelihood inference and model selection. *Biometrika*, 92(3), 519–528.
- Vautard, R., Kadygrov, N., Iles, C., Boberg, F., Buonomo, E., e Coauthors (2021). Evaluation of the large EURO-CORDEX regional climate model ensemble. *Journal of Geophysical Research: Atmospheres*, 126:e2019JD032344.
- Villarini, G., Smith, J.A., Baeck, M.L., Vitolo, R., Stephenson, D. B. & Krajewski, W.F. (2011) On the frequency of heavy rainfall for the Midwest of the United States. *Journal of Hydrology*, 400, 103–120.
- Wagner, S., Berg, P., Schaedler, G. & Kunstmann, H. (2013) High resolution regional climate model simulations for Germany: part II—projected climate changes. *Climate Dynamics*, 40, 415–427.
- Wang, C., Zhang, I., Lee, S.-k., Wu, L. & Mechoso, C.R. (2014) A global perspective on CMIP5 climate model biases. *Nature Climate Change*, 4, 201–205.
- Warrach-Sagi, K., Schwitalla, T., Wulfmeyer, V. & Bauer, H.S. (2013) Evaluation of a climate simulation in Europe based on the wrf-noah model system: precipitation in Germany. *Climate Dynamics*, 41(3), 755–774.
- Wasko, C., Sharma, A. & Westra, S. (2016) Reduced spatial extent of extreme storms at higher temperatures. *Geophysical Research Letters*, 43(8), 4026–4032.
- Westra, S. & Sisson, S.A. (2011) Detection of non-stationarity in precipitation extremes using a max-stable process model. *Journal of Hydrology*, 406(1–2), 119–128.
- Xu, H., Chen, H. & Wang, H. (2021) Detectable human influence on changes in precipitation extremes across China. *Earth's Futures*, 10(2), e2021EF002409.
- Yang, D., Kane, D., Zhang, Z., Legates, D. & Goodison, B. (2005) Bias corrections of long-term (1973–2004) daily precipitation data over the northern regions. *Geophysical Research Letters*, 32, L19501.
- Yang, L., Franzke, C.L.E. & Fu, Z. (2020a) Evaluation of the ability of regional climate models and a statistical model to represent the spatial characteristics of extreme precipitation. *International Journal of Climatology*, 40, 6612–6628.
- Yang, L., Franzke, C.L.E. & Fu, Z. (2020b) Power-law behaviour of hourly precipitation intensity and dry spell duration over the United States. *International Journal of Climatology*, 40(4), 2429–2444.
- Yang, Z. & Villarini, G. (2019) Examining the capability of reanalyses in capturing the temporal clustering of heavy precipitation across Europe. *Climate Dynamics*, 53(16), 1845–1857.
- Zeder, J. & Fischer, E.M. (2020) Observed extreme precipitation trends and scaling in Central Europe. *Weather and Climate Extremes*, 29, 100266.
- Zhang, X., Alexander, L., Hegerl, G., Jones, P., Tank, A., Peterson, T. et al. (2011) Indices for monitoring changes in extremes based on daily temperature and precipitation data. *WIREs Climate Change*, 2, 851–870.
- Zittis, G., Hadjinicolaou, P., Klangidou, M., Proestos, Y. & Lelieveld, J. (2019) A multi-model, multi-scenario, and multi-domain analysis of regional climate projections for the mediterranean. *Regional Environmental Change*, 19, 2621–2635.
- Zou, W., Yin, S. & Wang, W. (2021) Spatial interpolation of the extreme hourly precipitation at different return levels in the haihe river basin. *Journal of Hydrology*, 598, 126273.

**How to cite this article:** Yang, L., Franzke, C. L. E., & Duan, W. (2023). Evaluation and projections of extreme precipitation using a spatial extremes framework. *International Journal of Climatology*, 43(7), 3453–3475. <https://doi.org/10.1002/joc.8038>